

1 **THE CELL WALL OF *STREPTOCOCCUS PNEUMONIAE***

2

3 **Waldemar Vollmer¹, Orietta Massidda² and Alexander Tomasz³**

4

5

6 ¹ Institute for Cell and Molecular Biosciences, The Centre for Bacterial Cell Biology, Newcastle
7 University, Newcastle upon Tyne, United Kingdom.

8 ² Centre for Integrative Biology, University of Trento, Trento, Italy.

9 ³The Rockefeller University, New York, NY, USA.

10

11

12 **Summary**

13 *Streptococcus pneumoniae* has a complex cell wall that plays key roles in cell shape
14 maintenance, growth and cell division, and interactions with components of the human host. The
15 peptidoglycan has a heterogeneous composition with more than 50 different subunits
16 (muropeptides) – products of several peptidoglycan modifying enzymes. The amidation of
17 glutamate residues in the stem peptide is needed for efficient peptide cross-linking, and peptides
18 with a dipeptide branch prevail in some beta-lactam resistant strains. The glycan strands are
19 modified by deacetylation of N-acetylglucosamine residues and O-acetylation of N-
20 acetylmuramic acid residues, and both modifications contribute to pneumococcal resistance to
21 lysozyme. The glycan strands carry covalently attached wall teichoic acid and capsular
22 polysaccharide. Pneumococci are unique in that the wall teichoic acid and lipoteichoic acid
23 contain the same, unusually complex repeating units decorated with phosphoryl choline residues,
24 which anchor the choline-binding proteins. The structures of lipoteichoic acid and the attachment
25 site of wall teichoic acid to peptidoglycan have recently been revised. During growth
26 pneumococci assemble their cell wall at mid-cell in coordinated rounds of cell elongation and
27 division, leading to the typical ovococcal cell shape. Cell wall growth depends on the
28 cytoskeletal FtsA and FtsZ proteins and is regulated by several morphogenesis proteins that also
29 show patterns of dynamic localization at mid-cell. Some of the key regulators are phosphorylated
30 by StkP and dephosphorylated by PhpP, to facilitate robust selection of the division site and
31 plane, and maintain cell shape.

32

33 **Introduction**

34 Since the last edition of this book (Year 2006) a number of important publications
35 appeared in the literature the inclusion of which made it necessary to limit the topics of this
36 chapter to information that has bearing on the biochemical and genetic aspects of covalently
37 linked components of the pneumococcal cell wall. Information on proteins non-covalently
38 attached to the cell wall (Chapter 24); cell walls and phase variation (Chapter 22) and
39 inflammatory activity of cell walls (Chapter 21) are reviewed separately.

40 Historically, studies of the pneumococcal cell wall were motivated by such unique
41 features as the presence of choline in the teichoic acids and the pleiomorphic changes that
42 accompany removal or alteration of choline residues; and structural changes in peptidoglycan
43 that are associated with penicillin resistance. Most recent contributions to the field include
44 immunofluorescence (1-7) or fluorescent tagged (8, 9)(microscopic localization of cell wall
45 synthetic enzymes at sites of wall synthesis; identification of genetic determinants and enzymes
46 that are involved with the chemical modification of peptidoglycan precursors and peptidoglycan
47 itself, the synthesis of teichoic acid precursors and the assembly of lipoteichoic acid (LTA) and
48 wall teichoic acid (WTA); and the mechanisms and regulation of the cell wall machinery at the
49 central growth zone.

50

51 **Functional anatomy of pneumococcal cell wall.**

52 The overwhelming majority of “natural” isolates of pneumococci are enwrapped on their
53 outermost surface by one or the other of the more than 90 chemically different capsular
54 polysaccharides that this bacterial species is capable of synthesizing (10)).

55 Under these diverse structures lies the cell wall which, as far as the resolution of currently
56 used analytical techniques can tell, is much more uniform in its chemistry: it is composed of a
57 peptidoglycan covalently linked to chains of an unusually complex teichoic acid (11-13) which
58 contain as structural components phosphoryl choline residues (14, 15). The phosphoryl choline
59 residues play multiple roles in the physiology and virulence of the pneumococcus (see below).
60 The two polymers, peptidoglycan and teichoic acid, make up the bulk of the cell wall in roughly
61 equal (mg to mg) proportions (16). In most but not all cases, chains of the capsular
62 polysaccharide are attached by covalent bonds to the underlying peptidoglycan (17) (Fig. 1).

63 In electron microscopic thin sections (18) prepared by the method of Kellenberger
64 (osmium tetroxide and glutaraldehyde fixation followed by uranylacetate and lead citrate
65 staining) the cell wall of *Streptococcus pneumoniae* strain R36A appears as a band of uniform
66 width composed of two electron dense lines (30-40 nm each) enclosing a wider low density layer
67 (60-80 nm). The distribution of teichoic acid chains appears to be uniform within this wall layer
68 (19) and this is presumably also true for the peptidoglycan. Some anatomically differentiated
69 areas may be identified through electron microscopy. These are (i) the equatorial areas where
70 cell wall growth becomes centripetal (formation of septum or cross wall) and which represent the
71 “growth zones” of the entire wall; (ii) in dividing cells a circumferential thickening (“hump”) of
72 the cell wall appears at the place of the incipient septa. (iii) Parallel, or perhaps just prior to the
73 beginning of the formation of septum, the hump appears to be split at the center, and the two
74 halves begin to “move” on the cell surface symmetrically to the left and to the right of the
75 ingrowing septum coupled to the growth and eventual division of the cell into two daughter cells.
76 Due to the conservative mode of replication of the pneumococcal cell wall (see below), these two
77 half-humps are morphological age markers: they divide the cell wall of each pneumococcal cell

78 into two hemispheres which differ in age by one cell generation. The functional correlates of
79 these morphological changes began to be identified by the use of immunofluorescence
80 microscopy which allowed the localization of the various pneumococcal high molecular weight
81 penicillin binding proteins (PBPs) and the FtsZ-ring to equatorial and septal areas of the bacteria
82 in various stages of cell division (2-4, 7). A special role of two hydrolases, the carboxypeptidase
83 PBP3 (1, 20) and the endopeptidase PcsB (21-23) in these processes was also proposed. (iv) The
84 final stage of cell division: the separation of daughter cells may be inhibited in pneumococci by
85 several means resulting in the formation of long chains of bacteria. Under these conditions one
86 can observe by electron microscopy a thin bridge of cell wall material connecting neighboring
87 cells to one another. The hydrolase, LytB (an endo- β -1,4-N-acetylglucosaminidase) has been
88 identified as an enzyme essential for the terminal separation of daughter cells at the end of cell
89 division (24, 25).


90

91 **Structure of peptidoglycan.**

92 Purified cell walls of the non-encapsulated strain R6St (streptomycin-resistant) of
93 *Streptococcus pneumoniae* were hydrolyzed by the pneumococcal amidase (N-acetylmuramic
94 acid L-alanine amidase; the product of *lytA* gene) under conditions in which this enzyme can
95 quantitatively release the peptide units of cell wall muropeptides. A method that uses
96 muramidase digestion of the pneumococcal cell wall or peptidoglycan followed by HPLC
97 separation of muropeptides, through an adaptation of the method of Glauner and Schwarz, has
98 been described (26, 27).

99 In the amidase method, the family of peptides were separated by high performance liquid
100 chromatography (HPLC) and size fractionation; determination of amino acid composition and

101 NH₂ termini. Partial sequencing of the peptides generated by HPLC and analysis by time-of-
102 flight mass spectrometry has allowed the identification of a surprisingly large number of
103 monomeric, dimeric and trimeric peptides (28) showing a diversity comparable to that seen
104 among the mucopeptide species identified in *E. coli*. In the structural assignments it was assumed
105 that the amino acids within the stem peptides had the usual, alternating sequence of L and D
106 amino acids beginning with L-alanine in position 1, followed by a D-isoglutamine and then by L-
107 lysine. The carboxyterminus in the stem peptide is occupied by two consecutive D-alanine
108 residues; however, such mucopeptides with intact pentapeptide residue are rare in pneumococci
109 cultivated under normal growth conditions. Extension of this analytical technique to cell walls of
110 clinical isolates from a large variety of isolation sites and dates and expressing a variety of
111 different capsules has led to the proposition that the cell wall mucopeptide composition of *S.*
112 *pneumoniae* grown in the commonly-used semisynthetic media and harvested in the late
113 exponential phase is constant and characteristic of the species. The most abundant monomer of
114 the pneumococcal peptidoglycan was a tripeptide, the most frequent dimer a directly crosslinked
115 tri-tetrapeptide. Interestingly, the representation of carboxyterminal alanine was extremely rare
116 suggesting the presence of powerful DD- and LD-carboxypeptidases. These enzymes, PBP3 and
117 LdcB, will be discussed below.

118 An interesting feature of the peptide network was the presence of both directly and
119 indirectly crosslinked components. In the latter, alanyl-serine or alanyl-alanine dipeptides formed
120 the crosslink. In terms of crosslinking mode, the pneumococcal cell wall may be classified as
121 either A1 3 depending on which dimer one chooses. A massive distortion of peptidoglycan
122 composition in the direction of preponderance of indirectly crosslinked components was
123 demonstrated in several penicillin resistant clinical isolates (29).

124 The amidase also releases the glycan chains which in *S. pneumoniae* harbor two
125 modifications: *N*-deacetylation of some of the GlcNAc residues resulting in glucosamine, and O-
126 acetylation at some of the MurNAc residues. The latter modification is acid labile and lost during
127 the removal of wall teichoic acid to purify peptidoglycan and therefore the glycan chains
128 released by the amidase carry glucosamine residues the percentage of which depends on the
129 strain and growth conditions. The isolated glycan chains can be chemically re-acetylated and
130 analyzed by HPLC with or without partial digestion by muramidase. This analysis revealed that
131 glycan chains of less than 25 disaccharide units are virtually absent in pneumococcal PG (27), in
132 sharp contrast to that of staphylococci or *E. coli* in which short glycan chains prevail (30, 31).
133 That pneumococcal PG contains relatively long glycan chains was confirmed by size exclusion
134 chromatography (32).

135 The muramidase method in combination with mass spectrometry allowed detection of
136 ~50 different muropeptides (27). It confirmed the above mentioned peptide composition and
137 quantified the abundance of modifications in uncross-linked (monomeric) and cross-linked
138 (dimers, trimers) structures, allowing predictions about the activities of cell wall enzymes. For
139 example, non-amidated D-glutamate residues at position 2 were significantly less abundant in
140 cross-linked muropeptides, suggesting that enzymes performing cross-linking reactions (the
141 penicillin-binding proteins) require the presence of the amidated D-glutamate residue at position
142 2 (27, 33). The analysis also revealed the presence of cross-linked muropeptides (mainly trimers)
143 that lacked GlcNAc or the GlcNAc-MurNAc disaccharide at one of the peptides, indicating *N*-
144 acetylglucosaminidase and amidase activities, presumably those of LytB and LytA, respectively.
145 Muropeptide analysis has recently been used to study different aspects of pneumococcal cell wall
146 physiology (34-36).

147

148 **Peptidoglycan biosynthesis and remodeling**

149 Pneumococci contain the essential genes of the general biochemical pathway of
150 peptidoglycan synthesis and cell morphogenesis that were studied extensively in other model
151 species such as *E. coli* and *B. subtilis* (37, 38). Many of the peptidoglycan precursor genes and
152 cell division proteins cluster in three chromosomal regions, instead of one single cluster present
153 in *E. coli* and *B. subtilis*, consistent with the hypothesis that the ovoid shaped pneumococci
154 require less co-regulation of cell wall and division genes than rod-shaped species (39). In this
155 section we will focus on covalent modifications in the peptidoglycan that are important for the
156 physiology or lifestyle of pneumococci.

157

158 ***Modifications of the peptidoglycan precursor.***

159 Many Gram-positive species amidate the D-isoglutamate residue at the α -carboxylic
160 group by transfer of an amido group from L-glutamine to the cytosolic precursors UDP-
161 MurNAc-pentapeptide or the bactoprenol-linked precursors lipid I and lipid II. This amidation
162 reaction is catalyzed by a complex of two proteins, MurT and GatD, which were originally
163 identified in *S. aureus* (40). MurT/GatD are essential in both, *S. aureus* and *S. pneumoniae* (40,
164 41), consistent with the observation that amidation of the lipid II precursor is required for
165 efficient cross-linking in an *in vitro* assay for peptidoglycan synthesis with purified penicillin-
166 binding proteins (33). Hence, MurT/GatD seem to be essential because they provide a
167 modification needed for the essential peptide cross-linking reaction.

168 The presence of a 'branch' consisting of 2 to 7 L-amino acids "added" to the ϵ -amino
169 group of L-lysine at position 3 of the stem peptide is another wide-spread modification in Gram-

170 positive bacteria whereby the sequence of the branch varies between species. Virtually all *S.*
171 *aureus* strains have a pentaglycine branch but the peptidoglycan is less homogeneous in *S.*
172 *pneumoniae* in which strains can significantly differ in the amount of three types of peptides:
173 with no branch, with an L-Ala-L-Ala branch or with an L-Ser-L-Ala branch (42).

174 The branch is added to the lipid II precursor by the ligases MurM and MurN. The *in vivo*
175 substrate of MurM is lipid II and the enzyme catalyzes the addition of a serine or alanine residue
176 (depending on the particular *murM* allele) to the free amino group of lysine in the stem peptide –
177 in a reaction in which the amino acid donor is presumed to be an amino acyl-tRNA (43). This
178 reaction is followed by the MurM catalyzed addition of an alanine to complete the dipeptide
179 branch (see Fig. 2). Although the peptide branches synthesized by MurM and MurN are not
180 essential for pneumococcal growth, they are required in various strains to express high levels of
181 β -lactam resistance. A more detailed description of the connection between the *murMN* operon
182 and β -lactam resistance is provided in part 4 of this chapter (below).

183

184 ***Penicillin-binding proteins (PBPs)***

185 *S. pneumoniae* has six PBPs of which three, PBP1a, PBP1b and PBP2a are class A bi-
186 functional glycosyltransferase-transpeptidases (GTase-TPases) capable of polymerizing the
187 precursor lipid II to form the glycan chains and performing peptide cross-linking reactions. None
188 of these bi-functional enzymes is essential, but double mutants lacking *pbp1a* and *pbp2a* are not
189 viable (44), and *in vitro* experiments with the purified proteins showed that both require
190 amidated lipid II substrate for efficient transpeptidase activity (33).

191 *S. pneumoniae* also has two essential class B monofunctional transpeptidases, PBP2x and
192 PBP2b, involved with septal and peripheral peptidoglycan synthesis, respectively (7, 45).

193 Consistent with their roles, cells depleted of PBP2x become elongated and cells depleted of
194 PBP2b are shorter. PBP2x has two C-terminal PASTA (PBP and Serine/Threonine kinase
195 associated) domains which are required to localize the protein at mid-cell (46). Genetic evidence
196 points to an important role of branched peptide substrates for these PBPs. The remaining PBP,
197 PBP3, is not a synthase but a carboxypeptidase for trimming of pentapeptides to tetrapeptides
198 (see below).

199
200 ***Trimming of the peptides by carboxypeptidases.*** Newly synthesized peptidoglycan contains
201 abundant pentapeptides with a D-alanyl-D-alanine terminus, but these are trimmed in two steps
202 to tripeptides which prevail in the mature pneumococcal peptidoglycan. The DD-
203 carboxypeptidase PBP3 produces tetrapeptides (47), which are the substrate for the LD-
204 carboxypeptidase LdcB (or DacB) to produces the tripeptides. The wall peptide composition in a
205 PBP3 defective mutant (48) and in the laboratory strain R36A growing in the presence of sub-
206 inhibitory concentrations of clavulanic acid, a selective inhibitor of PBP3 in this bacterium (49)
207 showed accumulation of peptide species that retained carboxyterminal D-alanine residues.
208 Pneumococci grown in the presence of clavulanate also showed abnormal physiological
209 properties: premature induction of stationary phase autolysis; hypersensitivity to lysozyme and
210 reduced MIC values for deoxycholate and penicillin.

211 The *ldcB* gene was identified in a search for hypothetical peptidoglycan hydrolase genes,
212 and a deletion mutant has defects in cell shape and septation (50), as has a *dacA* mutant lacking
213 PBP3 (1). However, only *dacB* mutants were significantly attenuated in an intranasal mouse
214 infection model, and showed increased uptake by professional macrophages and reduced
215 adherence to lung epithelial cells (51). The *dacB* mutant is rich in tetrapeptides (50, 52), but it is

216 not known why the presence of tetrapeptides instead of tripeptides has these drastic effects on the
217 physiology and pathogenicity of pneumococci. The crystal structure of LdcB shows a catalytic
218 domain with a fold characteristic for the LAS family of Zn-dependent peptidases (51, 52).

219

220 ***The putative lytic transglycosylase MltG***

221 The *mltG* (*spd_1346*) gene was recently linked to peripheral peptidoglycan synthesis
222 based on the observation that its inactivation suppresses the requirement for PBP2b, MreCD,
223 RodA and RodZ, i.e., genes that are all part of the pneumococcal elongation machinery (53).
224 MltG has a YceG-family domain that ~~has been hypothesized to have~~ lytic transglycosylase
225 activity. A model has been proposed according to which MltG removes nascent glycan strands,
226 produced by PBP1a, from their membrane anchor to facilitate their incorporation into the old cell
227 wall by RodA and PBP2b (53). However, direct proof for a lytic transglycosylase activity of
228 MltG has yet to be presented, and the lytic transglycosylase products, 1,6-anhydro-*N*-
229 acetylmuramic acid termini in glycan chains and turnover products have yet to be detected.

230

231 ***Peptidoglycan hydrolases involved in septum remodeling and cleavage***

232 Several peptidoglycan hydrolases are important for pneumococcal growth and
233 morphology. The extracellular protein PcsB localizes to the cell division site where it is required
234 for proper septum formation and cleavage (54). The *pcsB* gene is the only essential gene under
235 the control of the WalRK cell wall stress regulon, and the depletion of *pcsB* results in growth
236 arrest and severe morphological defects. The active site of PcsB resides near the C-terminus and
237 belongs to the CHAP (for Cysteine, Histidine dependent amidohydrolase/peptidase) family of
238 peptidoglycan endopeptidases, but such an activity could only be observed for purified PcsB

239 when tested in an in-gel zymogram assay. In the cell, PcsB requires activation by the essential
240 membrane-bound ABC transporter-type FtsEX complex (54, 55). The crystal structure of PcsB
241 shows an inactive homodimer in which the V-shaped coiled-coil domain of each monomer
242 inserts into the active site groove of the other, explaining why this dimer form is inactive (23). It
243 was suggested that FtsEX utilizes ATP hydrolysis to induce conformational changes in the PcsB
244 dimer to unlock this mutual inhibition. However, the precise roles of FtsEX and PcsB in septum
245 formation and cleavage has yet to be established.

246 LytB is a secreted endo- β -*N*-acetylglucosaminidase with a choline-binding domain
247 consisting of 14-18 imperfect repeats, which direct the enzyme to the septum and cell pole
248 regions, followed by an SH3b peptidoglycan binding domain, a small carbohydrate-binding
249 domain with unknown function and a C-terminal catalytic domain (56). LytB functions at the
250 final stages of the division process to separate the daughter cells. Mutants lacking LytB grow in
251 deeply constricted chains of unseparated cells (57). Purified LytB is able to disperse chaining
252 cells of a *lytB* mutant. LytB cleaves at sites with fully acetylated GlcNAc residues and has
253 preference for monomeric peptides, suggesting a substrate assisted catalytic mechanism (25).

254 Apart from their role in cleavage of the septum and autolysis, peptidoglycan hydrolases
255 do not seem to be very active during pneumococcal growth in the laboratory. There is a
256 minimum of peptidoglycan turnover at the hemispherical regions with the old peptidoglycan
257 remaining virtually inert during growth (58, 59).

258

259

260 ***Peptidoglycan N-acetylglucosamine deacetylase PgdA***

261 An unusually high proportion of hexosamine units in the glycan strands of the
262 pneumococcal cell wall is not *N*-acetylated, explaining the resistance of this peptidoglycan to the
263 hydrolytic action of lysozyme, a muramidase that cleaves in the glycan backbone. A gene, *pgdA*,
264 was identified as encoding for the peptidoglycan *N*-acetylglucosamine deacetylase A with amino
265 acid sequence similarity to fungal chitin deacetylases and rhizobial NodB chitooligosaccharide
266 deacetylases (60). PgdA is a metal-dependent enzyme belonging to the family 4 carbohydrate
267 esterases. Its crystal structure shows a His-His-Asp catalytic triad in its active site (61, 62).
268 Pneumococci in which *pgdA* was inactivated produce fully *N*-acetylated glycan and become
269 hypersensitive to exogenous lysozyme in the stationary phase of growth. The *pgdA* gene may
270 contribute to pneumococcal virulence by providing protection against host lysozyme. A
271 pneumococcal strain expressing capsular type II with inactivated *pgdA* showed reduced virulence
272 in the mouse model of intraperitoneal infection (63).

273

274 ***Peptidoglycan O-acetyltransferase***

275 Many bacteria modify the C6-OH group of MurNAc residues in their peptidoglycan by
276 an O-acetyl group and this modification has been implied in the regulation of autolysins and
277 resistance to lysozyme (64). The pneumococcal *adr* gene encoding the O-acetyltransferase has
278 been initially identified in a mariner mutagenesis screen for increased sensitivity to penicillin in
279 the background of the resistant strain Pen6 (65). *Adr* mutant cells also show higher sensitivity to
280 lysozyme, and *Adr* shares sequence homology with the peptidoglycan O-acetyltransferase OatA
281 of *S. aureus* (66). Muropeptide analysis by HPLC and mass spectrometry showed that the *adr*
282 mutant lacked muropeptides with O-acetylated MurNAc residues, suggesting that *Adr* is the
283 pneumococcal peptidoglycan O-acetyltransferase. Recent work showed that peptidoglycan O-

284 acetylation by Adr occurs at mid-cell and that this modification protects the cell wall from
285 cleavage by the autolysin LytA (67).

286

287 ***Sortase A-dependent covalent attachment of proteins to the pneumococcal cell wall***

288 Most virulence related pneumococcal proteins studied so far were shown to be attached to
289 the cell surface through the choline residues of teichoic acids, and pneumococci have been
290 described as a paradigm for the display of virulence proteins through specific but noncovalent
291 associations with the cell surface (68). Such choline binding proteins include PspA; PsaA (see
292 Chapters 21 and 22); the enzyme phosphoryl choline esterase (69, 70); and LytA, in which a 20-
293 amino-acid repeat was shown to recognize choline residues in wall or membrane teichoic acids
294 (71). The observations described in this report demonstrate that the mechanism of surface display
295 of proteins does not depend on the choline binding paradigm alone; pneumococci also use
296 covalent anchoring for some surface proteins. Data available from the genome of *S. pneumoniae*
297 strain R6 (72) indicate that there are at least 23 proteins carrying the LPXTG motif and 15 of
298 these have this recognition sequence at the C terminus, as expected for proteins that are
299 processed by a typical sortase.

300 Inactivation of sortase gene *srtA* in *Streptococcus pneumoniae* strain R6 caused the
301 release of beta-galactosidase and neuraminidase A (NanA) from the cell wall into the
302 surrounding medium. Both of these surface proteins contain the LPXTG motif in the C-terminal
303 domain. Complementation with plasmid-borne *srtA* reversed protein release. Deletion of *murM*,
304 a gene involved in the branching of pneumococcal peptidoglycan, also caused partial release of
305 beta-galactosidase, suggesting preferential attachment of the protein to branched muropeptides in
306 the cell wall. Inactivation of *srtA* caused decreased adherence to human pharyngeal cells in vitro

307 but had no effect on the virulence of a capsular type III strain of *S. pneumoniae* in the mouse
308 intraperitoneal model. These observations suggest that similarly to other gram-positive bacteria
309 sortase-dependent display of proteins occurs in *S. pneumoniae* and that some of these proteins
310 may be involved in colonization of the human host (73).

311

312 **Peptidoglycan composition and penicillin resistance**

313 The first series of highly penicillin resistant clinical isolates examined by the HPLC
314 method were from South Africa. It was in these isolates that the mechanism of resistance,
315 namely reduction in antibiotic “affinity” of penicillin binding proteins (PBPs), was identified for
316 the first time (74). It was also in genetic crosses with these isolates used as DNA donors that the
317 stepwise nature of penicillin resistance (i.e., the sequential reduction in the penicillin affinity of
318 several high molecular weight PBPs in parallel with the gradually increasing penicillin MIC
319 value) was recognized (74).


320 Analysis of the penicillin resistant South African clinical isolates revealed that they
321 produced cell walls of a radically different composition from the one seen in the penicillin
322 susceptible and non-encapsulated laboratory isolate (75). When the HPLC analysis was extended
323 to the walls of several penicillin susceptible clinical isolates and several resistant strains (all but
324 one from South Africa), the striking shift towards indirectly crosslinked wall peptide
325 composition in the resistant isolates was fully confirmed. A link between resistance to penicillin
326 and abnormal wall composition was also suggested by the analysis of genetic crosses: a shift
327 towards the distorted wall composition of the resistant DNA donor was observed in genetic
328 transformants above certain MIC value. It was suggested that the anomalous wall peptide

329 composition reflected the altered substrate preference of the penicillin resistant PBPs, a shift
330 from the linear to the branched wall peptide precursors (75).

331

332 **The *murMN* operon**

333 A considerable clarification concerning determinants of cell wall structure and also its
334 relationship to penicillin resistance was obtained by the identification of the *murMN* operon
335 which encodes enzymes involved in the synthesis of branched structured muropeptides in the
336 pneumococcal peptidoglycan (42). The same determinants were also described independently
337 and named *fib* by another group (76). The *murMN* operon shows homology to the *femXAB* genes
338 of *S. aureus* which are involved with the addition of the pentaglycine branches to the epsilon
339 amino group of lysine residues in the staphylococcal peptidoglycan (77).

340 Inactivation of the *murM* operon or inactivation of the *murM* gene alone did not interfere
341 with growth of the bacteria but caused the production of a peptidoglycan composed exclusively
342 of linear  muropeptides. Another consequence of inactivation was the complete loss of the
343 penicillin resistant phenotype. Examination of a large number of *S. pneumoniae* clinical isolates
344 representing different genetic lineages has identified several distinct *murM* alleles carried by
345 penicillin resistant strains which also showed different and unique muropeptide composition in
346 their peptidoglycan (78). Analysis of the *murM* alleles from penicillin resistant isolates showed
347 that they differed from one another and from the *murM* carried by penicillin susceptible strains in
348 regions of considerable sequence diversity that were distributed as heterologous “patches” along
349 the *murM* gene sequence. Different *murM* alleles from several penicillin resistant *S. pneumoniae*
350 strains, each with a characteristic branched peptide composition were introduced on a plasmid
351 into a common penicillin susceptible laboratory strain. All transformants remained penicillin

352 susceptible but their cell wall composition changed in directions which corresponded to the
353 muropeptide pattern of the strain from which the *murM* allele was derived. This observation
354 suggests that the muropeptide composition of *S. pneumoniae* is determined by the particular
355 *murM* carried by the strain (43, 78) (Figs. 3A and B and Table 1).

356 The relationship between *murM* alleles and the penicillin resistant phenotype is less clear.
357 In genetic transformation of high level penicillin resistance it was shown that successful
358 expression of the resistant phenotype required that the transformants received not only the
359 particular mosaic *pbp* genes of the DNA donor but also the *murM* allele carried by the donor
360 strain (79). However, in other experiments the linkage between penicillin resistance and
361 abnormal wall composition was lost in transformation experiments in which the first round of
362 transformation was followed by a second backcross (80). Interestingly in this particular
363 experiment the penicillin resistant secondary transformants began to show “fitness” defects:
364 defective growth and premature autolysis in antibiotic free medium, similar to the defective
365 physiology observed in laboratory isolates of penicillin resistant pneumococci (81).

366 Genetic analysis and molecular modeling of the *murM* protein has identified amino acid
367 residues that appear to be critical for the specificity of this protein and also pinpointed domains
368 which interact with the aminoacyl tRNA and the bactoprenyl linked substrate of the *murM*
369 catalyzed reaction (82).

370

371 **Structure of wall teichoic acid (WTA) and lipoteichoic acid (LTA)**

372 *The pneumococcal C-polysaccharide and F-antigen.* In 1930, long before LTAs and
373 TAs had been discovered and defined, pneumococcal TA was described as pneumococcal C-
374 polysaccharide by Tillett and coworkers (83). Thirteen years later, pneumococcal LTA was

375 isolated by Goebel and his colleagues in 1943 and named lipocarbohydrate or pneumococcal F-
376 antigen owing to its fatty acid content and immunological properties (84). In these early studies,
377 a structural relationship between C-polysaccharide and lipocarbohydrate was suggested and in
378 contrast to the various strain-specific capsular polysaccharides, lipocarbohydrate and C-
379 polysaccharide were considered pneumococcal common antigens. This was confirmed by
380 serological methods which showed that all 90 known capsular types of *Streptococcus*
381 *pneumoniae* possess C-polysaccharide and F-antigen (19). The two polymers differ
382 immunologically, as Forssman antigenicity is associated with the LTA (85, 86). As shown by
383 immunoelectron microscopy, C-polysaccharide is uniformly distributed on both the inside and
384 outside of the cell walls, and LTA is located on the surface of the cytoplasmic membrane (12).

385 Choline, the surface signature of pneumococci, was identified as a component of TA and
386 LTA (14, 15). The complex structures of WTA and LTA could not be unraveled before modern
387 analytical techniques became available (87). In 1980, Jennings and coworkers published the first
388 complete structure of pneumococcal TA (11). The structure of pneumococcal LTA was clarified
389 in 1992 (85) and revised in 2013 (88), and subsequent reinvestigation of the WTA, isolated from
390 the same strain from which the LTA had been isolated, revealed that both polymers possess
391 identical chain structures (13, 82). The linkage structure of WTA to PG was recently established
392 (13), and all genes required for TA synthesis were predicted by sequence comparisons (89).

393

394 ***Structure of teichoic acid (TA) and Lipoteichoic acid (LTA).*** The chains of LTA and TA
395 contain 4 to 8 identical pseudo-pentasaccharide repeating units which consist of the rare
396 positively charged amino sugar 2-acetamido-4-amino-2,4,6-trideoxy-D-galactose (AATGal); D-
397 glucose; ribitol 5-phosphate; two N-acetyl-D-galactosaminy (GalNAc) residues and one or two

398 phosphocholine residues. Hydroxyl groups of ribitol can be substituted by D-alanine. The repeats
399 are joined together by an α -1,4 glycosidic linkage between AATGal and a GalNAc residue of the
400 adjacent repeat. The functionally important phosphocholine residues are phosphodiester-linked
401 to O6 of the N-acetyl-D-galactosaminyl residues. The number of phosphocholine residues per
402 repeat is strain specific: in LTA and WTA of strain R6 the majority of repeats carry two
403 phosphocholine residues, whereas most of the repeats in strain Rx1 are substituted with one (Fig.
404 4). Moreover, the terminal repeating unit of both WTA and LTA can occur with or without the
405 phosphocholine substitution at both GalNAc residues. The chain of LTA is β -1,3 glycosidically
406 linked via the AATGal residue to O3 α -D-Glcp(1-3)-diacylglycerol (Fig. 4).

407 Microheterogeneity of LTA became apparent by hydrophobic interaction chromatography
408 and mass spectrometry analysis (85, 88). The chain of LTA may vary in length between four and
409 eight repeats, with the range differing from sample to sample. On SDS-polyacrylamide gel
410 electrophoresis LTA yields a ladder-like pattern of up to six bands, each differing from the next
411 by one repeat. Species with one phosphocholine per repeat are distinguished from species with
412 two by higher mobility of the individual bands.

413 In addition to the unusual complexity of the chemical structure of TA, pneumococci are
414 also unique because their wall teichoic acid (WTA) and lipoteichoic acid (LTA) possess identical
415 repeat and chain structures, whereas in other gram-positive bacteria WTAs and LTAs are
416 structurally and biosynthetically distinct entities. In LTA and WTA the AATGal residues are of
417 conformational importance because the positively charged amino groups interact electrostatically
418 or by hydrogen bonding with the negatively charged phosphate groups on the adjacent glucosyl
419 residues (87, 90).

420 Pneumococcal WTA chains have been isolated with or without attached peptidoglycan
421 fragment and were shown to contain 4 to 8 repeating units (13, 27). WTA is linked to the
422 peptidoglycan by a phosphodiester bond to O6 of some of the MurNAc-residues which is
423 demonstrated by the release of MurN-6-*P* on HCl hydrolysis of cell walls (91) and of
424 muropeptides. It is estimated that – dependent on the particular strain – between 15% up to 30%
425 of the muramic acid residues carry WTA chains (16, 92). In other Gram-positive bacteria
426 connecting the WTA chain and muramic acid by a phosphodiester bond typically have a linkage
427 unit containing glycerophosphate or *N*-acetylmannosamine, but these components could not be
428 detected either in the hydrolysate of pneumococcal cell walls or in WTA-containing
429 muropeptides. Since no other sugar was found either, an acid-degradable sugar like AATGal
430 was suggested as a component of the linkage unit (87). Indeed, PG chains with attached WTA
431 could be isolated showing that the AATGal residue of the first repeating unit has an α -
432 configuration and is directly linked to MurNAc 6-phosphate (13).

433 **Synthesis of teichoic acids and modifications**

434 Although only few enzymes of the pneumococcal TA pathway have been biochemically
435 studied the complete pathway was deduced from bioinformatics analysis (89). Many TA genes
436 cluster in three genomic regions, called *lic1*, *lic2* and *lic3*. The *lic1* region contains genes
437 encoding components for the uptake of choline (LicB), the choline kinase LicA and the
438 cytidyltransferase LicC which produces CDP-choline. In addition, the *lic1* region encodes for
439 TarI and TarJ which synthesize CDP-ribitol (93). The adjacent *lic2* region contains the *tacF*
440 gene, encoding the putative TA flippase, and the *licD1/licD2* genes encoding
441 phosphotransferases for decoration of the TA subunits with phosphoryl choline residues. The
442 *lic3* region locates elsewhere on the chromosome and was identified by the presence of a gene,

443 called *licD3*, with sequence similarity to *licD1* and *licD2*, which is surrounded by four other
444 putative TA genes. LicD3 is most likely the phosphotransferase for the transfer of ribitol
445 phosphate during synthesis of the repeating unit, which involves eight additional enzymes that
446 synthesize the repeating unit linked to the carrier lipid bactoprenol phosphate. Presumably,
447 Spr1222 polymerizes the TA precursors to the nascent chains, which are still linked to the carrier
448 lipid, before these are flipped across the cytoplasmic membrane by TacF. Interestingly, TacF is
449 specific for choline-loaded TA precursor chains, ensuring that the mature TAs contains
450 phosphoryl choline residues (94).

451 After reaching the outer leaflet of the cytoplasmic membrane the TA chains are either
452 transferred to peptidoglycan to become WTA, or to the glycolipid to form the LTA. The transfer
453 to peptidoglycan is catalyzed by members of the LCP (LytR-CpsA-Psr) family of proteins, which
454 have been identified as phosphotransferases involved in cell wall assembly in Gram-positive
455 bacteria (95). The three LCP proteins of *S. pneumoniae* appear to have semi-redundant roles in
456 the attachment of capsular polysaccharides and WTA to C6-OH of MurNAc residues in
457 peptidoglycan (96). However, strain D39 and strains with serotype 8 and 31 link the capsule
458 polymer via a 1,6-glycosidic bond to GlcNAc residues of the peptidoglycan. Such linkage is
459 inconsistent with catalysis by LCP enzymes, indicating that the nature of the capsule attachment
460 enzyme is still elusive (97). In the case of LTA, it is the membrane protein TacL that transfers
461 the TA precursor chains onto the glycolipid anchor. Interestingly, mutants lacking *tacL* grow
462 normally under laboratory condition but show attenuated virulence in mouse models of acute
463 and/or systemic infections by *S. pneumoniae* (13).

464 Pneumococci contain a *dlt* operon the products of which are responsible for the
465 decoration of LTA and WTA repeating units with D-alanine residues, which are attached via an

466 ester linkage to OH groups in ribitol (98). This modification introduces positive charges to TAs
467 and thus increases resistance to cationic antimicrobial peptides. While *S. pneumoniae* strain D39
468 modifies its TAs by alanylation, this modification is not present in the laboratory strain R6 and in
469 strain TIGR4 due to mutations in the *dlt* operon rendering it non-functional.

470

471 ***Phosphoryl choline esterase – PCE – enzymatic removal of phosphoryl choline residues from***
472 ***the pneumococcal cell wall.*** The *pce* encoding for a teichoic acid phosphoryl choline esterase
473 (Pce) – an enzyme capable of removing phosphorylcholine residues from the cell wall teichoic
474 acid and lipoteichoic acid – was identified independently by two research groups (69, 70). Pce
475 carries an N-terminal signal sequence, contains a C-terminal choline-binding domain with 10
476 homologous repeating units similar to those found in other pneumococcal surface proteins. The
477 catalytic (phosphorylcholine esterase) activity is localized on the N-terminal part of the protein.
478 The mature protein was over-expressed in *Escherichia coli* and purified in a one-step procedure
479 by choline-affinity chromatography. The product of the enzymatic digestion of ³H-choline-
480 labelled cell walls was shown to be phosphorylcholine. Inactivation of the *pce* gene in *S.*
481 *pneumoniae* strains by insertion-duplication mutagenesis caused a unique change in colony
482 morphology and a striking increase in virulence of a capsular type III strain in the intraperitoneal
483 mouse model. Pce may be a regulatory element involved with the interaction of *S. pneumoniae*
484 with its human host. Sequence comparison indicates that PCE, the protein originally identified
485 through its unique enzymatic activity (99) is identical to choline binding protein E (CbpE) –
486 described by Masure and colleagues as a protein implicated in the attachment of pneumococci to
487 nasopharyngeal cells (100). The crystal structure of Pce shows a catalytic site with two zinc ions
488 and an elongated binding domain recognizing the phosphocholine residues of teichoic acid (101).

489
490
491
492
493
494
495
496
497
498
499
500
501
502
503
504
505
506
507
508
509
510
511

Multiple functions of cell wall choline residues

Nutritional requirement for choline. Choline is an essential growth factor for all natural isolates of pneumococci which have to import this nutrient from the growth medium (102). Choline may be replaced by other amino alcohols such as ethanolamine which can incorporate into LTA and TA at the same positions as phosphocholine but it can not replace phosphocholine functionally. Ethanolamine-grown cells show a number of striking abnormalities which include inhibition of cell separation (growth in long chains); inhibition of DNA uptake in genetic transformation; lack of autolysis during treatment with penicillin and other wall inhibitors and detergents (103); production of an “immature – enzymatically inactive – form of the autolytic enzyme LytA (104); production of a cell wall that cannot absorb LytA (105) and is completely resistant to the hydrolytic action of LytA (106). However, the requirement of LytA for built-in phosphocholine residues is no longer seen when solubilized cell wall polymers are degraded to muropeptides (12) or when the TA is removed from peptidoglycan (48). These observations may be interpreted to indicate that TA prevents the access of autolysin to its cell wall substrate and that this effect is overcome by binding of the enzyme to the phosphocholine residues.

There are several proteins in pneumococci – including LytA, LytB and LytC – that specifically recognize and bind to phosphocholine residues. These proteins contain distinct domains which are responsible for their specific biological activities, whereas the choline-binding domains are homologous and contain 6 to 10 choline-recognizing repeats of ~20 amino acids each. The structure of crystallized LytA and LytC and their interaction with choline residues in the cell wall has been described (107, 108).

512 ***Choline-independent strains.*** A choline-independent strain, R6Cho⁻, was recovered from a
513 heterologous cross with DNA from *Streptococcus oralis* (48). *S. oralis* also incorporates
514 phosphocholine into its cell wall TA, but, unlike pneumococci has no nutritional requirement for
515 choline. Other choline-independent strains, for example JY2190 and R6Chi are mutants
516 generated by serial passage of strains in chemically defined medium containing decreasing
517 concentrations of ethanolamine with each passage (94, 109). None of these strains had acquired
518 the capability to synthesize choline or ethanolamine because phosphorylated amino alcohols
519 could not be detected in TA and LTA. In spite of the absence of phosphocholine there was no
520 alteration either in the structure of LTA and TA or in cell wall composition, including the stem
521 peptide profile. Only the phosphate content of cell walls was reduced, consistent with the
522 absence of phosphocholine. In vivo, the lack of active autolysins became apparent by impaired
523 cell separation at the end of cell division and by resistance against stationary phase and
524 penicillin-induced lysis. Due to the absence of choline from LTA, PspA was lost into the
525 surrounding medium whereas, in spite of choline-free TA, the amidase was retained on the cells.
526 Both choline-independent strains retained the capacity to incorporate choline into teichoic acids:
527 when grown in the presence of choline, PspA was retained, cells separated normally, became
528 penicillin-sensitive, and phosphocholine was discovered on LTA and TA.

529 In the case of strain R6Chi and related strains, the nutritional requirement for choline was
530 explained by the loss of specificity of the teichoic acid flippase TacF for choline loaded TA
531 precursor chains (94). R6Chi contains a single point mutation in the *tacF* gene, rendering the
532 cells choline-independent. When growing in the presence of choline, R6Chi still incorporated
533 phosphocholine into its teichoic acids, suggesting that the mutated TacF can transport choline-
534 loaded and -unloaded TA precursor chains. The presence of the *tacF* mutation also allowed for

535 the deletion of otherwise essential choline utilization genes *licABC*, producing a strain that did
536 not incorporate choline into its cell wall even when growing in the presence of exogenous
537 choline. An encapsulated version of this mutant was used to demonstrate the crucial role of cell
538 wall choline residues in immune evasion (110).

539

540 **Cell growth regulation during the cell cycle**

541 *Growth zone and cell wall segregation.* Similarly to other streptococci, pneumococci
542 incorporate new cell wall units into the pre-existing wall material at a single growth zone located
543 at the cell equator (mid-cell). Both peptidoglycan and teichoic acids units and also capsular
544 polysaccharide (111) enter the pneumococcal surface at this growth zone which could be
545 visualized by exploiting the unique selectivity of a pneumococcal enzyme, the peptidoglycan
546 hydrolase LytA for choline-containing segments of the cell wall (58). Pneumococci require
547 choline for growth and the design of this experiment was based on the observation that the
548 choline component of the wall teichoic acid can be replaced by structural analogues such as
549 ethanolamine. Pneumococci grown in ethanolamine containing medium show several striking
550 abnormalities: unlike the choline grown bacteria, pneumococci utilizing ethanolamine grow in
551 long chains and are completely resistant to the cell wall degrading activity of LytA (103). Upon
552 addition of trace amounts of radiolabeled choline to a culture grown on ethanolamine the
553 bacteria immediately shifted to the utilization of choline so that the nascent wall units that began
554 to incorporate into the cell surface contained choline residues in the teichoic acid component of
555 the nascent cell wall and produced regions that were susceptible to hydrolysis by exogenous
556 LytA enzyme added to the medium. It was possible to show by electron microscopy that under
557 these conditions the LytA enzyme performed an enzymatic “microsurgery” on the bacteria: it

558 has selectively removed a thin equatorially located band of cell wall, thus identifying the
559 anatomical site of wall incorporation and growth zone (58).

560 Another abnormality of the ethanolamine-grown pneumococci, the complete inhibition of
561 cell separation, has allowed the design of experiments to test the mode of inheritance of
562 pneumococcal cell walls. Pneumococci labeled in their wall by titrated choline were shifted to an
563 ethanolamine-containing medium in which the bacteria continued to grow in the form of chains
564 of cells, i.e. “linear clones” in which the distribution of radioactively labeled bacteria could be
565 followed (by autoradiography) as a function of cell generations in the ethanolamine containing
566 medium. Since the teichoic acid choline does not exhibit turnover during growth, the localization
567 of radioactively labeled cells within the chains of bacteria could provide clues as to the mode of
568 wall segregation. The finding was that the radioactive label remained in large clusters in
569 association with cells that were located either at the tips or at the center of chains. The results
570 demonstrate the conservation of large hemispherical segments of the cell wall which are passed
571 on intact to daughter cells during cell division (112).

572 Novel methods such as staining of nascent peptidoglycan with fluorescent vancomycin
573 (113), incorporation of fluorescent D-amino acids (114) and super-resolution microscopy (32)
574 confirmed that pneumococci incorporate new cell wall units into the pre-existing wall material at
575 a single growth zone located at mid-cell.

576

577 **Cell wall growth and cell division complexes.** The mode of growth and cell wall segregation
578 described above implies that *S. pneumoniae*, as the model rods *Escherichia coli* and *B. subtilis*,
579 grows by alternating cycles of peripheral (side-wall) and septal peptidoglycan synthesis.
580 Consistent with this, the *S. pneumoniae* chromosome was found to encode proteins that are part

581 of the elongation machinery (elongasome), such as MreC, MreD, MltG, RodZ, RodA, PBP2b,
582 PBP1a and CozE, and others that are part of cell division machinery (divisome), such as FtsZ,
583 FtsA, ZapA, ZapB, EzrA, FtsE, FtsX, FtsK, FtsL, FtsB(DivIC), FtsQ(DivIC), SepF, GpsB,
584 DivIVA, FtsW, PBP1a, PBP2x, PcsB and LytB, as well as proteins that have a regulatory role in
585 these processes (4, 39, 53, 115-118).

586 Nevertheless, the characteristic ovococcal shape of pneumococci suggests that there must
587 be major differences in the cell wall growth mechanism compared to those of the rods. One
588 central difference is that pneumococci, despite conservation of all the other components of the
589 elongation complex lack the rod-shape determinant MreB, *i.e.* the actin-like protein that in rod-
590 shaped model bacteria provides the dynamic cytoskeletal scaffold to maintain rod-shape (119).
591 The second difference is that, despite previous reports (2), both components of the elongasome
592 and divisome show a clear septal localization, with no substantial variation in timing of
593 recruitment, although they may show differences in localization profile. The latter is best
594 reflected by the specific mid-cell localization of peptidoglycan synthases PBP2b and PBP2x,
595 which are involved with peripheral and septal cell wall growth, respectively (7). Importantly,
596 these differences from rods have led to the proposal that in *S. pneumoniae* and in other oval-
597 shaped cocci the elongation and septal machineries coexist in a single, intimately interconnected
598 and tightly regulated complex, or super-complex (Fig. 5) rather than in two separated ones (39,
599 115). Subsequent studies supported this model and provided insights into the coordination and
600 regulation of the complex during the cell cycle (120-123).

601 Information regarding gene essentiality among *S. pneumoniae* proteins involved in cell
602 growth and division have been available thanks to both global and dedicated studies. However, it
603 was not possible to assess directly the effect of inactivation of these genes until genetic systems

604 allowing the generation of merodiploids and conditional lethal mutants became available.
605 Moreover, a recent work employing a CRISPRi method (41) provides an additional powerful
606 tool to confirm results obtained with other methods and identify and characterize new essential
607 genes.

608 Genes encoding pneumococcal elongasome proteins were found to be essential in *S.*
609 *pneumoniae* D39 strain (53, 123, 124). However, some of these genes were not essential in strain
610 R6, a laboratory derivative of D39, and similar strains (53, 122-124). Presumably, these
611 laboratory strains contain pre-existing suppressor mutations that could compensate for the loss of
612 otherwise essential genes. Interestingly, inactivation of *mreC*, *mreD*, *mltG* and *rodZ* in *S.*
613 *pneumoniae* D39 are directly suppressed by mutations that inactivate *pbp1a* function or upon
614 *pbp1a* deletion (53, 124). Strain R6 contains an allelic variant of PBP1a (T124A D388E), the
615 functional importance of which has yet to be determined. In agreement, allele swapping
616 experiments showed that the *pbp1a* allele from R6 was sufficient to compensate for *mreCD* loss
617 in the R6 genetic background but less so in the D39 background, suggesting that other mutations
618 present in R6 must be involved in the strong suppression of *mreCD* essentiality (124). This result
619 is also supported by the fact that *pbp2a*, which shows a synthetic lethal relationship with *pbp1a*,
620 can be readily inactivated in strain R6 (44).

621 A previously uncharacterized gene, *spd_0768* (*spr0777* in R6) encoding the membrane
622 protein named CozE (for Coordinator of zonal elongation) was identified in a Tn-seq screen for
623 genes dispensable in D39 with inactivated *pbp1a* (118). Inactivation of *cozE* or *mreCD* in the
624 presence of PBP1a resulted in an aberrant relocalization of PBP1a and peptidoglycan synthesis
625 from mid-cell to the whole cell periphery and cells became increasingly spherical before they
626 lysed. Similarly to *mreCD*, *cozE* is dispensable in the R6 genetic background. CozE interacts

627 directly with MreCD and PBP1a. Together the results were interpreted as CozE being part of a
628 coordination mechanism, critical for proper zonal cell wall synthesis, by connecting PBP1a with
629 the other components of the elongation machinery *via* direct interactions (118).



630 With the exception of *pcsB* and *gpsB*, which showed strain-dependent essentiality,
631 inactivation of cell division genes were more consistent between strains. Of these, *ftsZ*, *ftsA*,
632 *ezrA*, *ftsEX*, *ftsL*, *ftsB* (*divIC*) and *pbp2x* were demonstrated to be essential in different
633 commonly used genetic backgrounds (7, 45, 46, 54, 121, 125).

634 As in other bacteria, in *S. pneumoniae* cell division starts with the localization of the
635 tubulin-like FtsZ and the actin-like FtsA cell division proteins (126) that assemble at mid-cell to
636 form the Z-ring required for the recruitment of the other components to complete cytokinesis.

637 Photoactivated localization microscopy (PALM) showed that as in other bacteria the Z-ring
638 in *S. pneumoniae* displayed a patchy structure rather than forming a homogenous ring, providing
639 important insight into its *in vivo* organization (127). Following the fluorescent tagged-FtsZ
640 localization and the Z-ring diameter, it was observed that FtsZ molecules assemble at mid-cell at
641 the beginning of the cell cycle to form a single patchy ring, that thickens and then disassembles
642 during constriction, while new Z-rings assemble at the future division sites (or new equators) of
643 the newborn cells. Notably, unconstricted double Z-rings, suggesting short-lived intermediates,
644 were observed in a small percentage of cells at mid-cell but not at the future division site (127).

645 Once the Z-ring is formed the later pneumococcal cell division proteins localize to mid-
646 cell, and a few to mid-cell and cell poles, in exponentially growing pneumococcal cells. A
647 hierarchical order of recruitment to the septum has not been determined and it may not even be a
648 linear sequence of events, albeit co-localization studies based on fluorescence microscopy
649 suggest that divisome assembly occurs in at least two steps. In the absence of MreB it is still

650 unknown how elongation components are targeted to mid-cell and how lateral and septal growth
651 are coordinated. FtsZ is believed to be the best candidate to act as a scaffold to coordinate both
652 side-wall and septal synthesis (127), although this role has not been experimentally verified, and
653 the effect on *S. pneumoniae* cells of depletion of essential proteins involved in the initial steps of
654 cell division were not available until recently.

655 A recent study characterized conditional lethal mutants for the cell division protein FtsA
656 providing insights about how integration of the elongation and septation machineries at a single
657 mid-cell location in *S. pneumoniae* may result in distinct cell growth pattern characteristic of
658 oval-shaped cocci. Unexpectedly, the complete depletion of FtsA in the pneumococcus resulted
659 in cell ballooning and ultimately lysis, in sharp contrast to the cell filamentation phenotype
660 observed in rods (121). FtsZ rings and peptidoglycan synthesis delocalized upon FtsA
661 inactivation, suggesting that the cells could neither elongate nor divide. In contrast, inactivation
662 of genes encoding other cell division components, such as GpsB (5   ~~et al., 2013~~) and SepF
663 (128), which in *B. subtilis* are synthetically lethal with *ftsA* (129, 130), resulted in enlarged and
664 elongated cells, with multiple FtsZ rings but not cell enlargement or lysis. Consistent with these
665 results, and in contrast to the model rods where FtsA localizes after FtsZ, in *S. pneumoniae* FtsZ
666 and FtsA are targeted to mid-cell at the earliest stages of the process and both form a ring that
667 remains co-localized throughout the cell cycle, while GpsB and SepF are recruited later, after the
668 Z-ring is assembled (121).

669 Taken together these observations led to the hypothesis that, in oval-shape cocci, the actin-
670 like FtsA, and not FtsZ, could play a major role in coordinating peripheral and septal
671 peptidoglycan synthesis, likely carrying out a similar role as the actin-like MreB in pre-septal
672 synthesis in *E. coli*. However, since FtsA is needed to tether FtsZ to the membrane (131) and

673 FtsZ may be required for FtsA to be targeted to the septum, additional work is necessary to
674 distinguish any direct role for FtsA in coordinating both modes of PG synthesis from that of
675 FtsZ.




676 While the elucidation of the mechanisms that in *S. pneumoniae* control the intimate
677 coordination between the two PG biosynthetic machineries still awaits further study, new
678 insights came from an unanticipated source, the screening for mutations that bypass the need of
679 PBP2b. This approach identified the membrane-bound ~~hypothetical~~ endo-lytic transglycosylase,
680 MltG (see above), which is involved in cell elongation (53). More recently, the inactivation of
681 two other genes, *spd_0675* and *spd_1849* (*spr0683* and *spr1851* in R6, respectively) was shown
682 to remove the requirement for PBP2b, MreCD, RodA, RodZ and GpsB in *S. pneumoniae* D39
683 (123). The corresponding proteins, named KhpA and KhpB, form an RNA-binding complex
684 which regulates cell division post-transcriptionally. Inactivation of *khpA* or *khpB* resulted in cells
685 with a significant reduction in cell volume, ~~but~~ they overall maintained a normal aspect-ratio,
686 while inducing a strong increase in the expression of the WalRK cell wall stress regulon and
687 modulating the level of FtsA through a post-transcriptional mechanism. Indeed, overproduction
688 of FtsA was found necessary and sufficient to compensate for the loss of PBP2b, MreC, MreD
689 and RodA, but not of Rod~~Z~~ GpsB, indicating that KhpAB must also regulate other genes in
690 addition to *ftsA* (123).

691 Two independent studies also identified Spr1851/Spd_1849, either as a novel substrate for
692 phosphorylation by the Ser/Thr protein kinase, StkP, in the laboratory strain *S. pneumoniae* Rx1
693 (132) or as a suppressor of *pbp2b* in the R704 derivative of laboratory strain R6 (133) and named
694 it Jag (for Jag-domain protein) or EloR (for Elongasome-regulating protein), respectively. Jag
695 was found to be phosphorylated at least at T89 (132). Experiments with null or phosphoablative

696 (T89A) alleles of *eloR* in the R704 strain revealed that both *pbp2b* and *rodA* could be deleted,
697 while its phosphomimetic form (T89D or T89E) could only be tolerated in strains that acquired
698 suppressor mutations in *mreC* and *rodZ* (133). In contrast, no phenotype was observed in either
699 KhpB phosphoablative or phosphomimetic derivatives in *S. pneumoniae* D39, indicating that
700 T89~P phosphorylation of KhpB is not necessary for its function in the ~~parent strain~~ (123).
701 Despite discrepancies between strains, these studies highlight the crucial yet complex role of
702 StkP in the regulation of pneumococcal cell cycle.

703
704 **Regulators of cell wall growth and division and role of phosphorylation.** Similarly to other
705 Gram-positive bacteria, *S. pneumoniae* possesses, in addition to ~~the~~ histidine kinase two
706 components system (TCSs), a conserved signaling system consisting of a Ser/Thr protein kinase,
707 StkP, and a cognate PP2C-type, phosphatase, PhpP (134, 135). StkP belongs to the subfamily of
708 eukaryotic-type Ser/Thr kinases, ESTKs, and consists of a cytoplasmic kinase domain, a
709 transmembrane region and a C-terminal part outside the cell made up of four PASTA domain
710 also found in PBP2x (136).


711 StkP acts as a dimer and forms a signaling pair with PhpP (137, 138). Several StkP
712 substrates playing a role in cell wall metabolism and cell division were identified to be
713 phosphorylated *in vivo* in a global study of the pneumococcal phosphoproteome (139). However,
714 only some of them have been confirmed to be specifically phosphorylated by StkP *in vitro* and/or
715 *in vivo*. These include the phosphoglucosamine mutase GlmM, the PG precursor biosynthesis
716 enzyme MurC, the cell division proteins DivIVA(135, 140-144) and the recently discovered
717 substrates MapZ/LocZ (120, 145) and Jag/EloR/KhpB (123, 132, 133). Although StkP is not
718 essential in *S. pneumoniae*, the multiple phenotypes of an *stkP* mutant suggested that it was

719 involved in the regulation of cell growth and cell division (140, 141), virulence, competence
720 (134) and stress resistance (146). It was later shown that both StkP and its cognate PhpP localize
721 to the division site with active peptidoglycan synthesis and that the PASTA domains of StkP
722 were required for its septal localization, indicating that they bind to newly synthesized and still
723 uncross-linked peptidoglycan chains *in vivo*. Inactivation of *stkP*, or overproduction of PhpP,
724 resulted in elongated cells with multiple and often unconstricted division rings, perturbed in cell
725 wall synthesis. In contrast, *S. pneumoniae* cells overproducing StkP, or lacking functional PhpP,
726 were significantly smaller and rounder (132, 143). These data indicate that StkP and PhpP play
727 an important role in coordinating cell wall synthesis during growth and division to achieve and
728 maintain the characteristic ovococcal shape. StkP was proposed to act as a molecular switch that,
729 through phosphorylation of key division substrates, signals the shift from peripheral to septal cell
730 wall synthesis (143)   A parallel study on the role of StkP in pneumococcal cell division partially
731 confirmed these results and proposed diverse functions for the different StkP domains in the R6
732 derived strain R800 (142). In this strain, deletion of the *stkP* gene or expression of a truncated
733 protein lacking the kinase domain (StkP-PASTA-TMH) resulted in round and chaining cells
734 rather than in elongated cells, while the elongated morphology was only observed in mutants
735 expressing a truncated protein lacking the PASTA domains (StkP-KD-TMH) or the catalytically
736 inactivated StkP(K42M) (142), in agreement with what was already reported for the *S.*
737 *pneumoniae* mutant StkP(K42R) and other *stkP* mutants lacking the PASTA domains obtained in
738 different genetic backgrounds (140, 141, 143). The round and chaining phenotype, connected
739 with the *stkP* deletion or truncation (142), was not observed in other studies and was interpreted
740 to be likely due to differences in genetic background, growth conditions  or to suppressor
741 mutations in that specific *stkP* null strains (39). To date, the molecular mechanisms of StkP's

742 regulatory function on its substrates is still unclear, although recent studies have reported some
743 advances in this direction.


744 In 2014, Fleurie *et al.* reported that the DivIVA paralog, GpsB, a putative component of
745 the pneumococcal cell elongation and cell division complex, was required for proper localization
746 and activation of StkP in the *S. pneumoniae* R6 derivative strain R800 (120). R800 cells deleted
747 for *gpsB* were viable but displayed an elongated and twisted-towels phenotype, more severe than
748 that previously reported for *S. pneumoniae* D39 cells depleted of *gpsB*, where this gene is
749 essential (5). Both FtsZ and PG synthesis were shown to have an helical pattern of localization in
750 Δ *gpsB* R800 cells, in which phosphorylation of all StkP substrates, including itself, was
751 abolished, consistent with the StkP delocalization observed. The R800 Δ *divIVA* phenotype,
752 instead, was consistent with the Δ *divIVA* phenotype previously reported for *S. pneumoniae* Rx1
753 strain (3); however its characteristic rounder and chainy morphology was reinterpreted as a
754 major defect in cell elongation (120) rather than a defect in septum closure and pole maturation
755 as originally proposed (3). In addition, *divIVA* inactivation was found to suppress the elongated
756 phenotype of Δ *gpsB* cells. Together these observations formed the basis for a model in which
757 DivIVA (required for cell elongation) and GpsB (required for cell division) constituted the
758 mechanism for the molecular switch to coordinate peripheral and septal PG synthesis, connecting
759 them to the Z-ring through the cell division protein EzrA: GpsB and DivIVA did not interact
760 directly with FtsZ but both interacted directly with EzrA, that in turn interacted with FtsZ (120).
761 In this model, GpsB, which has been shown to be phosphorylated in *S. agalactiae* (147) and *B.*
762 *subtilis* (148) but not in *S. pneumoniae*, would be needed for StkP localization at mid-cell and for
763 consequent phosphorylation of itself and its substrates, in particular DivIVA, to activate septum
764 closure. The elongated phenotype of the *S. pneumoniae* R800 cells expressing the

765 phosphoablative DivIVA allele T201A, the only amino acid residue of the protein shown to be
766 phosphorylated (142), further supported this interplay between GpsB, DivIVA and StkP.

767 In 2016, Straume *et al.* reported that *S. pneumoniae* R6 depleted for PBP2b, which grows
768 as long chains of characteristic lentil-shaped cells, has an altered stem peptide composition and is
769 hypersensitive to the peptidoglycan hydrolase CbpD, which is produced during competence (45).
770 They developed a genetic screen to identify genes that, when inactivated, would display a
771 PBP2b-like CbpD-dependent lytic phenotype, encoding proteins functionally related to PBP2b
772 (149). Four out of the 20 proteins tested, RodA, DivIVA, Spr0777 (later identified as
773 Spd_0768/CozE) and MreD (but not of MreC), showed a PBP2b-like competence-induced
774 autolytic response and consequently belong to the cell elongation complex (45). Intriguingly, this
775 study revealed that the *mreD* mutant differed from the expected morphology observed in other
776 studies for *mreD* mutants in the same or similar genetic backgrounds (39, 118, 124), highlighting
777 once more the difficulties to understand individual effects of gene inactivation in *S. pneumoniae*. 

778 The CbpD-dependent lysis data were then correlated with protein-protein interactions
779 between the identified proteins using the Bacterial Two-Hybrid Analysis (BACTH) system
780 (150). PBP2b interacted with RodA, confirming that these proteins have a close functional
781 relationship also in *S. pneumoniae*. Other interactions detected were between DivIVA and
782 PBP2b, DivIVA and Spr0777(CozE), and also the known DivIVA self-interaction (3, 149).

783 Taken together, these data were interpreted as DivIVA being part of, and required for,
784 proper localization of the pneumococcal elongasome, likely recruited by its interacting partner
785 CozE, supported by the observations that truncations determining the loss of DivIVA
786 localization were also associated with the loss of the elongasome function (149). However, direct
787 experimental proof for the lack of localization of DivIVA in the absence of CozE or known


788 components of the elongasome in the absence of DivIVA, is presently missing. Moreover,
789 $\Delta divIVA$ cells showed a significantly smaller increase in the amount of branched stem peptide
790 incorporated in the PG with respect to that of cells depleted for PBP2b, RodA or CozE (149). As
791 DivIVA is dispensable and shows a similar phenotype in all *S. pneumoniae* genetic backgrounds,
792 while other members of the elongation complex are not, a deeper understanding of the
793 localization profile and time of arrival at midcell of the different cell cycle proteins would be
794 needed to reveal their precise function. 

795 The regulatory function in cell wall biosynthesis of its paralog, GpsB, appears to become
796 more clear. Similar to DivIVA, GpsB, is also found in Gram-positive bacteria and contains a
797 conserved N-terminal domain, which recognizes the negative membrane curvature at the nascent
798 division septum (130, ~~151-153~~).

799 The *gpsB* gene is essential in *S. pneumoniae* D39 strain but not in its laboratory derivatives
800 R6 or R800 strains (5, 120). The recent work of Rued *et al.* (2017) showed that GpsB was not
801 strictly required for StkP localization or peptidoglycan synthesis at division septa. GpsB
802 depletion resulted in elongated cells with multiple Z-rings but no helical localization of FtsZ in
803 twisted-towels cells was observed. However, D39 cells depleted for GpsB showed decreased
804 StkP-mediated phosphorylation that could be suppressed by functional inactivation (mutation or
805 deletion) of its cognate PhpP phosphatase, which also relieved the cells from the need of GpsB.
806 A similar suppressor mutation inactivating PhpP was detected in $\Delta gpsB$ mutants obtained in the
807 other, commonly used, D39 laboratory derivative, Rx1(122). Importantly, GpsB forms a
808 complex with EzrA, MreC, StkP, PBP2a and PBP2x and directly interacts with some of these
809 proteins. Moreover, functional relationships were identified, based on synthetic lethality with
810 $\Delta pbp1a$ or $\Delta pbp2a$, with PBP2a and also with PBP2x, in which transpeptidase activity was

811 prevented from localizing at the center of division septa in the absence of GpsB (122). A
812 previous work reported that, although PBP2x is not an obvious StkP substrate, the two proteins
813 form a complex in the *S. pneumoniae* membrane and the PASTA domains of StkP interacted
814 directly with the extracellular region of PBP2x, likely allowing correct localization of both
815 protein at the division site (6).


816 Taken together, these results highlight a key role for GpsB in regulating the peripheral and
817 septal synthesis, through the regulation of PBP activities during the cell cycle, in agreement with
818 what is observed for other Gram-positive bacteria (154, 155). A revised model for GpsB function
819 would then be that, on one hand, GpsB activates PBP2a and StkP-PBP2x to close the septal ring
820 but, on the other hand, it negatively regulates peripheral elongation by inhibiting the activity of
821 PBP2b and MreC (122).

822 While these aspects of the function of GpsB are relatively well understood, the role of
823 phosphorylation for GpsB function is not. The recent studies on GpsB (120, 122) both agreed
824 that inactivation of GpsB reduces StkP-mediated phosphorylation and, consequently, that GpsB
825 is important for optimal phosphorylation. However, because GpsB does not appear to be a
826 substrate of StkP, the functional relationship between both proteins remains unclear. Hence,
827 whether StkP phosphorylates DivIVA as part of a molecular switch that together with GpsB and
828 StkP control peripheral vs. septal PG synthesis remains controversial. In contrast with what was
829 reported for the *S. pneumoniae* R800 strain (120), $\Delta divIVA$ mutations were not found to be
830 epistatic to $\Delta gpsB$ mutations in strains D39 and its derivatives R6 and Rx1 (122), and $\Delta divIVA$
831 cells did not show any detectable morphological phenotype when producing the phosphoablative
832 DivIVA T201A allele (122, 149), also different from what was observed in the *S. pneumoniae*
833 R800 strain (120, 142) (~~Fleurie *et al.*, 2012, Fleurie *et al.*, 2014~~). 

834



835 ***Division site selection (MapZ/LocZ) and origin of replication.*** Until recently, no mechanisms
836 for targeting FtsZ and the division complex to the nascent septum were identified and no
837 counterparts of the widespread or specific systems described in other bacteria, were found to be
838 present in *S. pneumoniae*. Rod-shaped model species use the Min system and nucleoid occlusion
839 to prevent asymmetric cell division and/or the septum from constricting over unsegregated
840 chromosomes but, in contrast to the striking conservation of the proteins that constitute the cell
841 elongation and division complexes, the proteins involved are poorly conserved reviewed in (156,
842 158).





843 It came as a surprise when two independent studies reported the characterization of a
844 previously unknown substrate of StkP, annotated as Spr0334 (SPD_0342 in D39) and showed
845 that a specific system for correctly identifying the midcell did indeed exist also in *S. pneumoniae*
846 (145, 159). The protein was named MapZ (for Mid-cell-anchored protein Z) (159) or LocZ (for
847 Localizing at the midcell of Z) (145), and shown to be a membrane protein consisting of a
848 cytoplasmic domain and two extracellular domains (EC) separated by a highly entropic serine-
849 rich region. MapZ/LocZ has a rather narrow phylogenetic distribution, being present only in
850 streptococci, enterococci and lactococci.



851 Consistent with its proposed function, MapZ/LocZ was found to localize as a ring at
852 midcell at the very early stages of cell division and before FtsZ (159) or FtsZ/FtsA (145).
853 ~~However, differently from any other cell division proteins, soon after its localization~~  MapZ/LocZ
854 splits into two rings that move away with the so called “wall bands” or “equatorial rings” until
855 they reach the equators of the newly forming daughter cells, marking the future division sites
856 (145, 159).

857 The gene encoding MapZ/LocZ was found to be dispensable in four different genetic
858 backgrounds, R800 (159), D39, R6 and Rx1 (145), and its deletion resulted in misshapen cells
859 often showing misplaced septa (145, 159). Moreover, in the absence of MapZ/LocZ, FtsZ (and
860 FtsA) rings formed but were not localized and/or correctly oriented with respect to the
861 longitudinal axis of the cells. A direct interaction between MapZ cytoplasmic domain and FtsZ
862 was detected and MapZ alleles lacking the N-terminal domain were unable to promote correct
863 FtsZ placement (159). Finally, both studies identified that MapZ/LocZ was phosphorylated by
864 StkP at Thr67 and Thr78 and that both phosphomimetic (T67-78E) and phosphoablative (T67-
865 78A) allelic variants localized to midcell, although the phenotypes of the strains differed
866 completely, ranging from severe defects in cell shape and viability with aberrant FtsZ structures
867 and reduced number of Z-ring per cell (159) to no evident morphological defects and a wild-type
868 morphology (145).

869 Thus, albeit the overall conclusions of the MapZ/LocZ studies agreed on the protein
870 function, the two works differed in important details: (i) the growth and morphological defects
871 are significantly more severe in the R800 background than in the others; (ii) in R800 there is a
872 third MapZ ring forming at mid-cell after the initial ring splits into two and moved apart from the
873 cell center, but this was not seen for LocZ in other strains; (iii) in R800, FtsZ was reported to
874 ~~move together with the MapZ rings to the future division site, whereas in the other strains FtsZ~~
875 ~~disassembles from mid-cell to assemble *de novo* at the future division site.~~ While these issues
876 need to be clarified, further analysis of MapZ, using both a genetic and a structural approach,
877 demonstrated the importance of the second EC domain, which shows a marked flexibility at acid
878 pH, while demonstrating that the first EC domain is likely a molecular scaffold or pedestal,
879 required to mark the division site (160).

880 A more recent study indicated that MapZ/LocZ is not involved in division site selection,
881 but rather in the selection of the correct division plane and that the replication status and the
882 position of the chromosome have, instead, a crucial impact on spatial regulation of cell division.
883 In particular, the position of the chromosome origin of replication precedes MapZ/LocZ at
884 midcell and promotes the use of the correct division site (161). These conclusions were based on
885 the reasoning that $\Delta mapZ/\Delta locZ$ mutants are not elongated, but rather shorter and with only
886 minor changes in cell morphology with respect to wild-type cells. Advanced fluorescent
887 microscopy and image analysis showed that FtsZ localization is not affected in cells lacking
888 MapZ, suggesting that it would not be ~~not~~   critical for accurate timing of the Z-ring assembly at
889 midcell (161). The localization profile of MapZ/LocZ during the cell cycle was consistent with
890 previous reports, however two and not three MapZ-rings were observed, in line with what was
891 previously observed for *S. pneumoniae* D39 and related derivatives (145) and not for *S.*
892 *pneumoniae* R800 (159).

893 The reported mislocalization of FtsZ in $\Delta mapZ/\Delta locZ$ cells was attributed to the FtsZ
894 fusion protein used in the previous studies to determine   Z localization in the null mutants (145,
895 159). ~~However, caution should be taken when using   ent tags.~~ This consideration applies
896 only to the MapZ study, where a GFP-FtsZ fusion used was the only source of FtsZ in the cell
897 (159) but not to the LocZ study, where the CFP-FtsZ fusion was ectopically produced, in
898 addition to native FtsZ (145). Nevertheless, the $\Delta mapZ/\Delta locZ$ phenotype was reinterpreted in a
899 new light and suggested that MapZ/LocZ could function in cell wall remodeling rather than in
900 site selection, similarly to peptidoglycan hydrolases and LMW-PBPs (161). However, this
901 intriguing hypothesis awaits experimental validation.

902 In conclusion, the study of the cell cycle of *S. pneumoniae* has benefited greatly from the
903 work on other organisms, in particular the model rods with which the pneumococcus has many
904 similarities as well as many marked differences. The gap in knowledge between *S. pneumoniae*
905 and the model organisms is rapidly closing and it will be interesting to see how further works
906 develop. Regulation of the cell cycle through phosphorylation is a relatively new and active area
907 of research (162) that will likely provide new insights on how *S. pneumoniae* succeeded to
908 manage peripheral and septal growth that emanates from a single insertion site located at the cell
909 center or mid-cell.  

910

911

912 **REFERENCES**

- 913 1. Morlot C, Noirclerc-Savoie M, Zapun A, Dideberg O, Vernet T. 2004. The D,D-
914 carboxypeptidase PBP3 organizes the division process of *Streptococcus pneumoniae*. Mol
915 Microbiol 51:1641-8.
- 916 2. Morlot C, Zapun A, Dideberg O, Vernet T. 2003. Growth and division of *Streptococcus*
917 *pneumoniae*: localization of the high molecular weight penicillin-binding proteins during the cell
918 cycle. Mol Microbiol 50:845-55.
- 919 3. Fadda D, Santona A, D'Ulisse V, Ghelardini P, Ennas MG, Whalen MB, Massidda O.
920 2007. *Streptococcus pneumoniae* DivIVA: localization and interactions in a MinCD-free context.
921 J Bacteriol 189:1288-98.
- 922 4. Zapun A, Vernet T, Pinho MG. 2008. The different shapes of cocci. FEMS Microbiol
923 Rev 32:345-60.
- 924 5. Land AD, Tsui HC, Kocaoglu O, Vella SA, Shaw SL, Keen SK, Sham LT, Carlson EE,
925 Winkler ME. 2013. Requirement of essential Pbp2x and GpsB for septal ring closure in
926 *Streptococcus pneumoniae* D39. Mol Microbiol 90:939-55.
- 927 6. Morlot C, Bayle L, Jacq M, Fleurie A, Tourcier G, Galisson F, Vernet T, Grangeasse C,
928 Di Guilmi AM. 2013. Interaction of Penicillin-Binding Protein 2x and Ser/Thr protein kinase
929 StkP, two key players in *Streptococcus pneumoniae* R6 morphogenesis. Mol Microbiol 90:88-
930 102.
- 931 7. Tsui HT, Boersma MJ, Vella SA, Kocaoglu O, Kuru E, Peceny JK, Carlson EE,
932 VanNieuwenhze MS, Brun YV, Shaw SL, Winkler ME. 2014. Pbp2x localizes separately from
933 Pbp2b and other peptidoglycan synthesis proteins during later stages of cell division of
934 *Streptococcus pneumoniae* D39. Mol Microbiol 94:21-40.

- 935 8. Eberhardt A, Wu LJ, Errington J, Vollmer W, Veening JW. 2009. Cellular localization of
936 choline-utilization proteins in *Streptococcus pneumoniae* using novel fluorescent reporter
937 systems. *Mol Microbiol* 74:395-408.
- 938 9. Henriques MX, Catalao MJ, Figueiredo J, Gomes JP, Filipe SR. 2013. Construction of
939 improved tools for protein localization studies in *Streptococcus pneumoniae*. *PLoS One*
940 8:e55049.
- 941 10. Kamerling JP. 2000. Pneumococcal Polysaccharides: A Chemical View, p 81-114. In
942 Tomasz A (ed), *Streptococcus pneumoniae*, Molecular Biology & Mechanisms of Disease.
943 Mary Ann Liebert, Inc, Larchmont, New York.
- 944 11. Jennings HJ, Lugowski C, Young NM. 1980. Structure of the complex polysaccharide C-
945 substance from *Streptococcus pneumoniae* type 1. *Biochemistry* 19:4712-9.
- 946 12. Sorensen UB, Henrichsen J. 1987. Cross-reactions between pneumococci and other
947 streptococci due to C polysaccharide and F antigen. *J Clin Microbiol* 25:1854-9.
- 948 13. Hess N, Waldow F, Kohler TP, Rohde M, Kreikemeyer B, Gomez-Mejia A, Hain T,
949 Schwudke D, Vollmer W, Hammerschmidt S, Gisch N. 2017. Lipoteichoic acid deficiency
950 permits normal growth but impairs virulence of *Streptococcus pneumoniae*. *Nat Commun*
951 8:2093.
- 952 14. Tomasz A. 1967. Choline in the cell wall of a bacterium: novel type of polymer-linked
953 choline in *Pneumococcus*. *Science* 157:694-7.
- 954 15. Brundish DE, Baddiley J. 1968. Pneumococcal C-substance, a ribitol teichoic acid
955 containing choline phosphate. *Biochem J* 110:573-82.

- 956 16. Mosser JL, Tomasz A. 1970. Choline-containing teichoic acid as a structural component
957 of pneumococcal cell wall and its role in sensitivity to lysis by an autolytic enzyme. *J Biol Chem*
958 245:287-98.
- 959 17. Bentley SD, Aanensen DM, Mavroidi A, Saunders D, Rabinowitsch E, Collins M,
960 Donohoe K, Harris D, Murphy L, Quail MA, Samuel G, Skovsted IC, Kalltoft MS, Barrell B,
961 Reeves PR, Parkhill J, Spratt BG. 2006. Genetic analysis of the capsular biosynthetic locus from
962 all 90 pneumococcal serotypes. *PLoS Genet* 2:e31.
- 963 18. Tomasz A. 2000. *Streptococcus pneumoniae*: Functional anatomy., p 9-21. In Tomasz A
964 (ed), *Streptococcus pneumoniae*: Molecular biology and Mechanisms of Disease - Update for the
965 1990s. Mary Ann Liebert, Inc, New York.
- 966 19. Skov Sorensen UB, Blom J, Birch-Andersen A, Henrichsen J. 1988. Ultrastructural
967 localization of capsules, cell wall polysaccharide, cell wall proteins, and F antigen in
968 pneumococci. *Infect Immun* 56:1890-6.
- 969 20. Schuster C, Dobrinski B, Hakenbeck R. 1990. Unusual septum formation in
970 *Streptococcus pneumoniae* mutants with an alteration in the D,D-carboxypeptidase penicillin-
971 binding protein 3. *J Bacteriol* 172:6499-505.
- 972 21. Ng WL, Kazmierczak KM, Winkler ME. 2004. Defective cell wall synthesis in
973 *Streptococcus pneumoniae* R6 depleted for the essential PcsB putative murein hydrolase or the
974 VicR (YycF) response regulator. *Mol Microbiol* 53:1161-75.
- 975 22. Barendt SM, Land AD, Sham LT, Ng WL, Tsui HC, Arnold RJ, Winkler ME. 2009.
976 Influences of capsule on cell shape and chain formation of wild-type and pcsB mutants of
977 serotype 2 *Streptococcus pneumoniae*. *J Bacteriol* 191:3024-40.

- 978 23. Bartual SG, Straume D, Stamsas GA, Munoz IG, Alfonso C, Martinez-Ripoll M,
979 Havarstein LS, Hermoso JA. 2014. Structural basis of PcsB-mediated cell separation in
980 *Streptococcus pneumoniae*. Nat Commun 5:3842.
- 981 24. Garcia P, Gonzalez MP, Garcia E, Lopez R, Garcia JL. 1999. LytB, a novel
982 pneumococcal murein hydrolase essential for cell separation. Mol Microbiol 31:1275-81.
- 983 25. Rico-Lastres P, Diez-Martinez R, Iglesias-Bexiga M, Bustamante N, Aldridge C, Heseck
984 D, Lee M, Mobashery S, Gray J, Vollmer W, Garcia P, Menendez M. 2015. Substrate
985 recognition and catalysis by LytB, a pneumococcal peptidoglycan hydrolase involved in
986 virulence. Sci Rep 5:16198.
- 987 26. Hakenbeck R, Konig A, Kern I, van der Linden M, Keck W, Billot-Klein D, Legrand R,
988 Schoot B, Gutmann L. 1998. Acquisition of five high-Mr penicillin-binding protein variants
989 during transfer of high-level beta-lactam resistance from *Streptococcus mitis* to *Streptococcus*
990 *pneumoniae*. J Bacteriol 180:1831-40.
- 991 27. Bui NK, Eberhardt A, Vollmer D, Kern T, Bougault C, Tomasz A, Simorre JP, Vollmer
992 W. 2012. Isolation and analysis of cell wall components from *Streptococcus pneumoniae*. Anal
993 Biochem 421:657-66.
- 994 28. Garcia-Bustos JF, Chait BT, Tomasz A. 1987. Structure of the peptide network of
995 pneumococcal peptidoglycan. J Biol Chem 262:15400-5.
- 996 29. Severin A, Tomasz A. 1996. Naturally occurring peptidoglycan variants of *Streptococcus*
997 *pneumoniae*. J Bacteriol 178:168-74.
- 998 30. Harz H, Burgdorf K, Holtje JV. 1990. Isolation and separation of the glycan strands from
999 murein of *Escherichia coli* by reversed-phase high-performance liquid chromatography. Anal
1000 Biochem 190:120-8.

- 1001 31. Boneca IG, Huang ZH, Gage DA, Tomasz A. 2000. Characterization of *Staphylococcus*
1002 *aureus* cell wall glycan strands, evidence for a new beta-N-acetylglucosaminidase activity. J Biol
1003 Chem 275:9910-8.
- 1004 32. Wheeler R, Mesnage S, Boneca IG, Hobbs JK, Foster SJ. 2011. Super-resolution
1005 microscopy reveals cell wall dynamics and peptidoglycan architecture in ovococcal bacteria. Mol
1006 Microbiol 82:1096-109.
- 1007 33. Zapun A, Philippe J, Abrahams KA, Signor L, Roper DI, Breukink E, Vernet T. 2013. In
1008 vitro reconstitution of peptidoglycan assembly from the Gram-positive pathogen *Streptococcus*
1009 *pneumoniae*. ACS Chem Biol 8:2688-96.
- 1010 34. Johnston C, Bootsma HJ, Aldridge C, Manuse S, Gisch N, Schwudke D, Hermans PW,
1011 Grangeasse C, Polard P, Vollmer W, Claverys JP. 2015. Co-inactivation of GlnR and CodY
1012 regulators impacts pneumococcal cell wall physiology. PLoS One 10:e0123702.
- 1013 35. Schweizer I, Blattner S, Maurer P, Peters K, Vollmer D, Vollmer W, Hakenbeck R,
1014 Denapaite D. 2017. New aspects of the interplay between Penicillin-binding proteins, MurM, and
1015 the two-component system CiaRH of Penicillin-resistant *Streptococcus pneumoniae* Serotype
1016 19A Isolates from Hungary. Antimicrob Agents Chemother 61.
- 1017 36. Todorova K, Maurer P, Rieger M, Becker T, Bui NK, Gray J, Vollmer W, Hakenbeck R.
1018 2015. Transfer of penicillin resistance from *Streptococcus oralis* to *Streptococcus pneumoniae*
1019 identifies *murE* as resistance determinant. Mol Microbiol 97:866-80.
- 1020 37. den Blaauwen T, de Pedro MA, Nguyen-Disteche M, Ayala JA. 2008. Morphogenesis of
1021 rod-shaped sacculi. FEMS Microbiol Rev 32:321-44.
- 1022 38. Typas A, Banzhaf M, Gross CA, Vollmer W. 2011. From the regulation of peptidoglycan
1023 synthesis to bacterial growth and morphology. Nat Rev Microbiol 10:123-36.

- 1024 39. Massidda O, Novakova L, Vollmer W. 2013. From models to pathogens: how much have
1025 we learned about *Streptococcus pneumoniae* cell division? Environ Microbiol 15:3133-57.
- 1026 40. Figueiredo TA, Sobral RG, Ludovice AM, Almeida JM, Bui NK, Vollmer W, de
1027 Lencastre H, Tomasz A. 2012. Identification of genetic determinants and enzymes involved with
1028 the amidation of glutamic acid residues in the peptidoglycan of *Staphylococcus aureus*. PLoS
1029 Pathog 8:e1002508.
- 1030 41. Liu X, Gally C, Kjos M, Domenech A, Slager J, van Kessel SP, Knoops K, Sorg RA,
1031 Zhang JR, Veening JW. 2017. High-throughput CRISPRi phenotyping identifies new essential
1032 genes in *Streptococcus pneumoniae*. Mol Syst Biol 13:931.
- 1033 42. Filipe SR, Pinho MG, Tomasz A. 2000. Characterization of the murMN operon involved
1034 in the synthesis of branched peptidoglycan peptides in *Streptococcus pneumoniae*. J Biol Chem
1035 275:27768-74.
- 1036 43. Filipe SR, Severina E, Tomasz A. 2001. Functional analysis of *Streptococcus*
1037 *pneumoniae* MurM reveals the region responsible for its specificity in the synthesis of branched
1038 cell wall peptides. J Biol Chem 276:39618-28.
- 1039 44. Paik J, Kern I, Lurz R, Hakenbeck R. 1999. Mutational analysis of the *Streptococcus*
1040 *pneumoniae* bimodular class A penicillin-binding proteins. J Bacteriol 181:3852-6.
- 1041 45. Berg KH, Stamsas GA, Straume D, Havarstein LS. 2013. Effects of low PBP2b levels on
1042 cell morphology and peptidoglycan composition in *Streptococcus pneumoniae* R6. J Bacteriol
1043 195:4342-54.
- 1044 46. Peters K, Schweizer I, Beilharz K, Stahlmann C, Veening JW, Hakenbeck R, Denapaite
1045 D. 2014. *Streptococcus pneumoniae* PBP2x mid-cell localization requires the C-terminal PASTA
1046 domains and is essential for cell shape maintenance. Mol Microbiol 92:733-55.

- 1047 47. Morlot C, Pernot L, Le Gouellec A, Di Guilmi AM, Vernet T, Dideberg O, Dessen A.
1048 2005. Crystal structure of a peptidoglycan synthesis regulatory factor (PBP3) from *Streptococcus*
1049 *pneumoniae*. J Biol Chem 280:15984-91.
- 1050 48. Severin A, Horne D, Tomasz A. 1997a. Autolysis and cell wall degradation in a choline-
1051 independent strain of *Streptococcus pneumoniae*. Microb Drug Resist 3:391-400.
- 1052 49. Severin A, Severina E, Tomasz A. 1997. Abnormal physiological properties and altered
1053 cell wall composition in *Streptococcus pneumoniae* grown in the presence of clavulanic acid.
1054 Antimicrob Agents Chemother 41:504-10.
- 1055 50. Barendt SM, Sham LT, Winkler ME. 2011. Characterization of mutants deficient in the
1056 L,D-carboxypeptidase (DacB) and WalRK (VicRK) regulon, involved in peptidoglycan
1057 maturation of *Streptococcus pneumoniae* serotype 2 strain D39. J Bacteriol 193:2290-300.
- 1058 51. Abdullah MR, Gutierrez-Fernandez J, Pribyl T, Gisch N, Saleh M, Rohde M, Petruschka
1059 L, Burchhardt G, Schwudke D, Hermoso JA, Hammerschmidt S. 2014. Structure of the
1060 pneumococcal l,d-carboxypeptidase DacB and pathophysiological effects of disabled cell wall
1061 hydrolases DacA and DacB. Mol Microbiol 93:1183-206.
- 1062 52. Hoyland CN, Aldridge C, Cleverley RM, Duchene MC, Minasov G, Onopriyenko O,
1063 Sidiq K, Stogios PJ, Anderson WF, Daniel RA, Savchenko A, Vollmer W, Lewis RJ. 2014.
1064 Structure of the LdcB LD-carboxypeptidase reveals the molecular basis of peptidoglycan
1065 recognition. Structure 22:949-60.
- 1066 53. Tsui HC, Zheng JJ, Magallon AN, Ryan JD, Yunck R, Rued BE, Bernhardt TG, Winkler
1067 ME. 2016. Suppression of a deletion mutation in the gene encoding essential PBP2b reveals a
1068 new lytic transglycosylase involved in peripheral peptidoglycan synthesis in *Streptococcus*
1069 *pneumoniae* D39. Mol Microbiol 100:1039-65.

- 1070 54. Sham LT, Barendt SM, Kopecky KE, Winkler ME. 2011. Essential PcsB putative
1071 peptidoglycan hydrolase interacts with the essential FtsXSpn cell division protein in
1072 *Streptococcus pneumoniae* D39. Proc Natl Acad Sci U S A 108:E1061-9.
- 1073 55. Sham LT, Jensen KR, Bruce KE, Winkler ME. 2013. Involvement of FtsE ATPase and
1074 FtsX extracellular loops 1 and 2 in FtsEX-PcsB complex function in cell division of
1075 *Streptococcus pneumoniae* D39. MBio 4.
- 1076 56. Bai XH, Chen HJ, Jiang YL, Wen Z, Huang Y, Cheng W, Li Q, Qi L, Zhang JR, Chen Y,
1077 Zhou CZ. 2014. Structure of pneumococcal peptidoglycan hydrolase LytB reveals insights into
1078 the bacterial cell wall remodeling and pathogenesis. J Biol Chem 289:23403-16.
- 1079 57. De Las Rivas B, Garcia JL, Lopez R, Garcia P. 2002. Purification and polar localization
1080 of pneumococcal LytB, a putative endo-beta-N-acetylglucosaminidase: the chain-dispersing
1081 murein hydrolase. J Bacteriol 184:4988-5000.
- 1082 58. Laitinen H, Tomasz A. 1990. Changes in composition of peptidoglycan during maturation
1083 of the cell wall in pneumococci. J Bacteriol 172:5961-7.
- 1084 59. Boersma MJ, Kuru E, Rittichier JT, VanNieuwenhze MS, Brun YV, Winkler ME. 2015.
1085 Minimal Peptidoglycan (PG) Turnover in wild-type and PG hydrolase and cell division mutants
1086 of *Streptococcus pneumoniae* D39 growing planktonically and in host-relevant biofilms. J
1087 Bacteriol 197:3472-85.
- 1088 60. Vollmer W, Tomasz A. 2000. The *pgdA* gene encodes for a peptidoglycan N-
1089 acetylglucosamine deacetylase in *Streptococcus pneumoniae*. J Biol Chem 275:20496-501.
- 1090 61. Blair DE, Schuttelkopf AW, MacRae JI, van Aalten DM. 2005. Structure and metal-
1091 dependent mechanism of peptidoglycan deacetylase, a streptococcal virulence factor. Proc Natl
1092 Acad Sci U S A 102:15429-34.

- 1093 62. Bui NK, Turk S, Buckenmaier S, Stevenson-Jones F, Zeuch B, Gobec S, Vollmer W.
1094 2011. Development of screening assays and discovery of initial inhibitors of pneumococcal
1095 peptidoglycan deacetylase PgdA. *Biochem Pharmacol* 82:43-52.
- 1096 63. Vollmer W, Tomasz A. 2002. Peptidoglycan N-acetylglucosamine deacetylase, a putative
1097 virulence factor in *Streptococcus pneumoniae*. *Infect Immun* 70:7176-8.
- 1098 64. Vollmer W. 2008. Structural variation in the glycan strands of bacterial peptidoglycan.
1099 *FEMS Microbiol Rev* 32:287-306.
- 1100 65. Crisostomo MI, Vollmer W, Kharat AS, Inhulsen S, Gehre F, Buckenmaier S, Tomasz A.
1101 2006. Attenuation of penicillin resistance in a peptidoglycan O-acetyl transferase mutant of
1102 *Streptococcus pneumoniae*. *Mol Microbiol* 61:1497-509.
- 1103 66. Bera A, Herbert S, Jakob A, Vollmer W, Gotz F. 2005. Why are pathogenic
1104 staphylococci so lysozyme resistant? The peptidoglycan O-acetyltransferase OatA is the major
1105 determinant for lysozyme resistance of *Staphylococcus aureus*. *Mol Microbiol* 55:778-87.
- 1106 67. Bonnet J, Durmort C, Jacq M, Mortier-Barriere I, Campo N, VanNieuwenhze MS, Brun
1107 YV, Arthaud C, Gallet B, Moriscot C, Morlot C, Vernet T, Di Guilmi AM. 2017. Peptidoglycan
1108 O-acetylation is functionally related to cell wall biosynthesis and cell division in *Streptococcus*
1109 *pneumoniae*. *Mol Microbiol* 106:832-846.
- 1110 68. Cossart P, Jonquieres R. 2000. Sortase, a universal target for therapeutic agents against
1111 gram-positive bacteria? *Proc Natl Acad Sci U S A* 97:5013-5.
- 1112 69. de las Rivas B, Garcia JL, Lopez R, Garcia P. 2001. Molecular characterization of the
1113 pneumococcal teichoic acid phosphorylcholine esterase. *Microb Drug Resist* 7:213-22.
- 1114 70. Vollmer W, Tomasz A. 2001. Identification of the teichoic acid phosphorylcholine
1115 esterase in *Streptococcus pneumoniae*. *Mol Microbiol* 39:1610-22.

- 1116 71. Garcia JL, Sanchez-Beato AR, Medrano FJ, Lopez R. 2000. Versatility of choline-
1117 binding domain, p 231-244. In Tomasz A (ed), *Streptococcus pneumoniae: Molecular Biology &*
1118 *Mechanisms of Disease*. Mary Ann Liebert, Inc, Larchmont, NY.
- 1119 72. Hoskins J, Alborn WE, Jr., Arnold J, Blaszcak LC, Burgett S, DeHoff BS, Estrem ST,
1120 Fritz L, Fu DJ, Fuller W, Geringer C, Gilmour R, Glass JS, Khoja H, Kraft AR, Lagace RE,
1121 LeBlanc DJ, Lee LN, Lefkowitz EJ, Lu J, Matsushima P, McAhren SM, McHenney M,
1122 McLeaster K, Mundy CW, Nicas TI, Norris FH, O'Gara M, Peery RB, Robertson GT, Rockey P,
1123 Sun PM, Winkler ME, Yang Y, Young-Bellido M, Zhao G, Zook CA, Baltz RH, Jaskunas SR,
1124 Rosteck PR, Jr., Skatrud PL, Glass JI. 2001. Genome of the bacterium *Streptococcus*
1125 *pneumoniae* strain R6. *J Bacteriol* 183:5709-17.
- 1126 73. Kharat AS, Tomasz A. 2003. Inactivation of the *srtA* gene affects localization of surface
1127 proteins and decreases adhesion of *Streptococcus pneumoniae* to human pharyngeal cells in
1128 vitro. *Infect Immun* 71:2758-65.
- 1129 74. Zigelboim S, Tomasz A. 1980. Penicillin-binding proteins of multiply antibiotic-
1130 resistant South African strains of *Streptococcus pneumoniae*. *Antimicrob Agents Chemother*
1131 17:434-42.
- 1132 75. Garcia-Bustos J, Tomasz A. 1990. A biological price of antibiotic resistance: major
1133 changes in the peptidoglycan structure of penicillin-resistant pneumococci. *Proc Natl Acad Sci U*
1134 *S A* 87:5415-9.
- 1135 76. Weber B, Ehlert K, Diehl A, Reichmann P, Labischinski H, Hakenbeck R. 2000. The *fib*
1136 locus in *Streptococcus pneumoniae* is required for peptidoglycan crosslinking and PBP-mediated
1137 beta-lactam resistance. *FEMS Microbiol Lett* 188:81-5.

- 1138 77. Rohrer S, Berger-Bachi B. 2003. FemABX peptidyl transferases: a link between
1139 branched-chain cell wall peptide formation and beta-lactam resistance in gram-positive cocci.
1140 Antimicrob Agents Chemother 47:837-46.
- 1141 78. Filipe SR, Severina E, Tomasz A. 2000. Distribution of the mosaic structured *murM*
1142 genes among natural populations of *Streptococcus pneumoniae*. J Bacteriol 182:6798-805.
- 1143 79. Smith AM, Klugman KP. 2000. Non-Penicillin-Binding protein mediated high-level
1144 penicillin and cephalosporin resistance in a Hungarian clone of *Streptococcus pneumoniae*.
1145 Microb Drug Resist 6:105-10.
- 1146 80. Severin A, Figueiredo AM, Tomasz A. 1996. Separation of abnormal cell wall
1147 composition from penicillin resistance through genetic transformation of *Streptococcus*
1148 *pneumoniae*. J Bacteriol 178:1788-92.
- 1149 81. Severin A, Vaz Pato MV, Sa Figueiredo AM, Tomasz A. 1995. Drastic changes in the
1150 peptidoglycan composition of penicillin resistant laboratory mutants of *Streptococcus*
1151 *pneumoniae*. FEMS Microbiol Lett 130:31-5.
- 1152 82. Fiser A, Filipe SR, Tomasz A. 2003. Cell wall branches, penicillin resistance and the
1153 secrets of the MurM protein. Trends Microbiol 11:547-53.
- 1154 83. Tillett WS, Goebel WF, Avery OT. 1930. Chemical and immunological properties of a
1155 species-specific carbohydrate of pneumococci. J Exp Med 52:895-900.
- 1156 84. Goebel WF, Shedlovsky T, Lavin GI, Adams MH. 1943. The heterophile antigen of
1157 pneumococcus. J Biol Chem 148:1-15.
- 1158 85. Behr T, Fischer W, Peter-Katalinic J, Egge H. 1992. The structure of pneumococcal
1159 lipoteichoic acid. Improved preparation, chemical and mass spectrometric studies. Eur J
1160 Biochem 207:1063-75.

- 1161 86. Briles EB, Tomasz A. 1975. Membrane lipoteichoic acid is not a precursor to wall
1162 teichoic acid in pneumococci. *J Bacteriol* 122:335-7.
- 1163 87. Fischer W. 1990. Bacterial phosphoglycolipids and lipoteichoic acids, p 123-234. In (ed)
1164 MK (ed), *Glycolipids, Phosphoglycolipids, and Sulfoglycolipids*, Vol 6 of DJ Hanahan (ed)
1165 *Handbook of Lipid Research*, vol 6. Plenum Press, New York.
- 1166 88. Gisch N, Kohler T, Ulmer AJ, Muthing J, Pribyl T, Fischer K, Lindner B,
1167 Hammerschmidt S, Zahringer U. 2013. Structural reevaluation of *Streptococcus pneumoniae*
1168 lipoteichoic acid and new insights into its immunostimulatory potency. *J Biol Chem* 288:15654-
1169 67.
- 1170 89. Denapate D, Bruckner R, Hakenbeck R, Vollmer W. 2012. Biosynthesis of teichoic acids
1171 in *Streptococcus pneumoniae* and closely related species: lessons from genomes. *Microb Drug*
1172 *Resist* 18:344-58.
- 1173 90. Klein RA, Hartmann R, Egge H, Behr T, Fischer W. 1996. The aqueous solution structure
1174 of a lipoteichoic acid from *Streptococcus pneumoniae* strain R6 containing 2,4-diamino-2,4,6-
1175 trideoxy-galactose: evidence for conformational mobility of the galactopyranose ring. *Carbohydr*
1176 *Res* 281:79-98.
- 1177 91. Liu TY, Gotschlich EC. 1967. Muramic acid phosphate as a component of the
1178 mucopeptide of Gram-positive bacteria. *J Biol Chem* 242:471-6.
- 1179 92. Garcia P, Garcia JL, Garcia E, Lopez R. 1989. Purification and characterization of the
1180 autolytic glycosidase of *Streptococcus pneumoniae*. *Biochem Biophys Res Commun* 158:251-6.
- 1181 93. Baur S, Marles-Wright J, Buckenmaier S, Lewis RJ, Vollmer W. 2009. Synthesis of
1182 CDP-activated ribitol for teichoic acid precursors in *Streptococcus pneumoniae*. *J Bacteriol*
1183 191:1200-10.

- 1184 94. Damjanovic M, Kharat AS, Eberhardt A, Tomasz A, Vollmer W. 2007. The essential
1185 *tacF* gene is responsible for the choline-dependent growth phenotype of *Streptococcus*
1186 *pneumoniae*. *J Bacteriol* 189:7105-11.
- 1187 95. Kawai Y, Marles-Wright J, Cleverley RM, Emmins R, Ishikawa S, Kuwano M, Heinz N,
1188 Bui NK, Hoyland CN, Ogasawara N, Lewis RJ, Vollmer W, Daniel RA, Errington J. 2011. A
1189 widespread family of bacterial cell wall assembly proteins. *EMBO J* 30:4931-41.
- 1190 96. Eberhardt A, Hoyland CN, Vollmer D, Bisle S, Cleverley RM, Johnsborg O, Havarstein
1191 LS, Lewis RJ, Vollmer W. 2012. Attachment of capsular polysaccharide to the cell wall in
1192 *Streptococcus pneumoniae*. *Microb Drug Resist* 18:240-55.
- 1193 97. Larson TR, Yother J. 2017. *Streptococcus pneumoniae* capsular polysaccharide is linked
1194 to peptidoglycan via a direct glycosidic bond to beta-D-N-acetylglucosamine. *Proc Natl Acad*
1195 *Sci U S A* 114:5695-5700.
- 1196 98. Kovacs M, Halfmann A, Fedtke I, Heintz M, Peschel A, Vollmer W, Hakenbeck R,
1197 Bruckner R. 2006. A functional *dlt* operon, encoding proteins required for incorporation of d-
1198 alanine in teichoic acids in gram-positive bacteria, confers resistance to cationic antimicrobial
1199 peptides in *Streptococcus pneumoniae*. *J Bacteriol* 188:5797-805.
- 1200 99. Holtje JV, Tomasz A. 1974. Teichoic acid phosphorylcholine esterase. A novel enzyme
1201 activity in pneumococcus. *J Biol Chem* 249:7032-4.
- 1202 100. Gosink KK, Mann ER, Guglielmo C, Tuomanen EI, Masure HR. 2000. Role of novel
1203 choline binding proteins in virulence of *Streptococcus pneumoniae*. *Infect Immun* 68:5690-5.
- 1204 101. Hermoso JA, Lagartera L, Gonzalez A, Stelter M, Garcia P, Martinez-Ripoll M, Garcia
1205 JL, Menendez M. 2005. Insights into pneumococcal pathogenesis from the crystal structure of
1206 the modular teichoic acid phosphorylcholine esterase Pce. *Nat Struct Mol Biol* 12:533-8.

- 1207 102. Rane L, Subbarow Y. 1940. Nutritional requirements of the pneumococcus: I. Growth
1208 factors for types I, II, V, VII, VIII. *J Bacteriol* 40:695-704.
- 1209 103. Tomasz A. 1968. Biological consequences of the replacement of choline by ethanolamine
1210 in the cell wall of *Pneumococcus*: chain formation, loss of transformability, and loss of autolysis.
1211 *Proc Natl Acad Sci U S A* 59:86-93.
- 1212 104. Lopez R, Garcia E, Garcia P, Garcia JL. 2000. The pneumococcal cell wall degrading
1213 enzymes: a modular desing to create new lysins?, p 197-211. In Tomasz A (ed), *Streptococcus*
1214 *pneumoniae*, Molecular Biology & Mechanisms of Disease. Mary Ann Liebert, Larchmond,
1215 New York.
- 1216 105. Giudicelli S, Tomasz A. 1984. Attachment of pneumococcal autolysin to wall teichoic
1217 acids, an essential step in enzymatic wall degradation. *J Bacteriol* 158:1188-90.
- 1218 106. Holtje JV, Tomasz A. 1975. Specific recognition of choline residues in the cell wall
1219 teichoic acid by the N-acetylmuramyl-L-alanine amidase of *Pneumococcus*. *J Biol Chem*
1220 250:6072-6.
- 1221 107. Fernandez-Tornero C, Garcia E, Lopez R, Gimenez-Gallego G, Romero A. 2002. Two
1222 new crystal forms of the choline-binding domain of the major pneumococcal autolysin: insights
1223 into the dynamics of the active homodimer. *J Mol Biol* 321:163-73.
- 1224 108. Perez-Dorado I, Gonzalez A, Morales M, Sanles R, Striker W, Vollmer W, Mobashery S,
1225 Garcia JL, Martinez-Ripoll M, Garcia P, Hermoso JA. 2010. Insights into pneumococcal
1226 fratricide from the crystal structures of the modular killing factor LytC. *Nat Struct Mol Biol*
1227 17:576-81.

- 1228 109. Yother J, Leopold K, White J, Fischer W. 1998. Generation and properties of a
1229 *Streptococcus pneumoniae* mutant which does not require choline or analogs for growth. J
1230 Bacteriol 180:2093-101.
- 1231 110. Gehre F, Spisek R, Kharat AS, Matthews P, Kukreja A, Anthony RM, Dhodapkar MV,
1232 Vollmer W, Tomasz A. 2009. Role of teichoic acid choline moieties in the virulence of
1233 *Streptococcus pneumoniae*. Infect Immun 77:2824-31.
- 1234 111. Wagner M. 1964. [Studies with fluorescent antibodies of growing bacteria. I.
1235 Regeneration of the cell wall in *Diplococcus pneumoniae*]. Zentralbl Bakteriolog Orig 195:87-93.
- 1236 112. Briles EB, Tomasz A. 1970. Radioautographic evidence for equatorial wall growth in a
1237 gram-positive bacterium. Segregation of choline-³H-labeled teichoic acid. J Cell Biol 47:786-90.
- 1238 113. Daniel RA, Errington J. 2003. Control of cell morphogenesis in bacteria: two distinct
1239 ways to make a rod-shaped cell. Cell 113:767-76.
- 1240 114. Kuru E, Hughes HV, Brown PJ, Hall E, Tekkam S, Cava F, de Pedro MA, Brun YV,
1241 VanNieuwenhze MS. 2012. In Situ probing of newly synthesized peptidoglycan in live bacteria
1242 with fluorescent D-amino acids. Angew Chem Int Ed Engl 51:12519-23.
- 1243 115. Sham LT, Tsui HC, Land AD, Barendt SM, Winkler ME. 2012. Recent advances in
1244 pneumococcal peptidoglycan biosynthesis suggest new vaccine and antimicrobial targets. Curr
1245 Opin Microbiol 15:194-203.
- 1246 116. Pinho MG, Kjos M, Veening JW. 2013. How to get (a)round: mechanisms controlling
1247 growth and division of coccoid bacteria. Nat Rev Microbiol 11:601-14.
- 1248 117. Philippe J, Vernet T, Zapun A. 2014. The elongation of ovococci. Microb Drug Resist
1249 20:215-21.

1250 118. Fenton AK, Mortaji LE, Lau DT, Rudner DZ, Bernhardt TG. 2017. CozE is a member of
1251 the MreCD complex that directs cell elongation in *Streptococcus pneumoniae*. Nat Microbiol
1252 2:16237.

1253 119. Busiek KK, Margolin W. 2015. Bacterial actin and tubulin homologs in cell growth and
1254 division. Curr Biol 25:R243-54.

1255 120. Fleurie A, Manuse S, Zhao C, Campo N, Cluzel C, Lavergne JP, Freton C, Combet C,
1256 Guiral S, Soufi B, Macek B, Kuru E, VanNieuwenhze MS, Brun YV, Di Guilmi AM, Claverys
1257 JP, Galinier A, Grangeasse C. 2014a. Interplay of the serine/threonine-kinase StkP and the
1258 paralogs DivIVA and GpsB in pneumococcal cell elongation and division. PLoS Genet
1259 10:e1004275.

1260 121. Mura A, Fadda D, Perez AJ, Danforth ML, Musu D, Rico AI, Krupka M, Denapaite D,
1261 Tsui HT, Winkler ME, Branny P, Vicente M, Margolin W, Massidda O. 2016. Roles of the
1262 essential protein FtsA in cell growth and division in *Streptococcus pneumoniae*. J Bacteriol
1263 doi:10.1128/JB.00608-16.

1264 122. Rued BE, Zheng JJ, Mura A, Tsui HT, Boersma MJ, Mazny JL, Corona F, Perez AJ,
1265 Fadda D, Doubravova L, Buriankova K, Branny P, Massidda O, Winkler ME. 2017. Suppression
1266 and synthetic-lethal genetic relationships of Δ *gpsB* mutations indicate that GpsB mediates
1267 protein phosphorylation and penicillin-binding protein interactions in *Streptococcus pneumoniae*
1268 D39. Mol Microbiol 103:931-957.

1269 123. Zheng JJ, Perez AJ, Tsui HT, Massidda O, Winkler ME. 2017. Absence of the KhpA and
1270 KhpB (JAG/EloR) RNA-binding proteins suppresses the requirement for PBP2b by
1271 overproduction of FtsA in *Streptococcus pneumoniae* D39. Mol Microbiol 106:793-814.

- 1272 124. Land AD, Winkler ME. 2011. The requirement for pneumococcal MreC and MreD is
1273 relieved by inactivation of the gene encoding PBP1a. *J Bacteriol* 193:4166-79.
- 1274 125. Le Gouellec A, Roux L, Fadda D, Massidda O, Vernet T, Zapun A. 2008. Roles of
1275 pneumococcal DivIB in cell division. *J Bacteriol* 190:4501-11.
- 1276 126. Lara B, Rico AI, Petruzzelli S, Santona A, Dumas J, Biton J, Vicente M, Mingorance J,
1277 Massidda O. 2005. Cell division in cocci: localization and properties of the *Streptococcus*
1278 *pneumoniae* FtsA protein. *Mol Microbiol* 55:699-711.
- 1279 127. Jacq M, Adam V, Bourgeois D, Moriscot C, Di Guilmi AM, Vernet T, Morlot C. 2015.
1280 Remodeling of the Z-Ring Nanostructure during the *Streptococcus pneumoniae* cell cycle
1281 revealed by photoactivated localization microscopy. *MBio* 6.
- 1282 128. Fadda D, Pischedda C, Caldara F, Whalen MB, Anderluzzi D, Domenici E, Massidda O.
1283 2003. Characterization of divIVA and other genes located in the chromosomal region
1284 downstream of the *dcw* cluster in *Streptococcus pneumoniae*. *J Bacteriol* 185:6209-14.
- 1285 129. Ishikawa S, Kawai Y, Hiramatsu K, Kuwano M, Ogasawara N. 2006. A new FtsZ-
1286 interacting protein, YlmF, complements the activity of FtsA during progression of cell division
1287 in *Bacillus subtilis*. *Mol Microbiol* 60:1364-80.
- 1288 130. Tavares JR, de Souza RF, Meira GL, Gueiros-Filho FJ. 2008. Cytological
1289 characterization of YpsB, a novel component of the *Bacillus subtilis* divisome. *J Bacteriol*
1290 190:7096-107.
- 1291 131. Krupka M, Cabre EJ, Jimenez M, Rivas G, Rico AI, Vicente M. 2014. Role of the FtsA C
1292 terminus as a switch for polymerization and membrane association. *MBio* 5:e02221.
- 1293 132. Ulrych A, Holeckova N, Goldova J, Doubravova L, Benada O, Kofronova O, Halada P,
1294 Branny P. 2016. Characterization of pneumococcal Ser/Thr protein phosphatase phpP mutant

1295 and identification of a novel PhpP substrate, putative RNA binding protein Jag. BMC Microbiol
1296 16:247.

1297 133. Stamsas GA, Straume D, Ruud Winther A, Kjos M, Frantzen CA, Havarstein LS. 2017.
1298 Identification of EloR (Spr1851) as a regulator of cell elongation in *Streptococcus pneumoniae*.
1299 Mol Microbiol 105:954-967.

1300 134. Echenique J, Kadioglu A, Romao S, Andrew PW, Trombe MC. 2004. Protein
1301 serine/threonine kinase StkP positively controls virulence and competence in *Streptococcus*
1302 *pneumoniae*. Infect Immun 72:2434-7.


1303 135. Novakova L, Saskova L, Pallova P, Janecek J, Novotna J, Ulrych A, Echenique J,
1304 Trombe MC, Branny P. 2005. Characterization of a eukaryotic type serine/threonine protein
1305 kinase and protein phosphatase of *Streptococcus pneumoniae* and identification of kinase
1306 substrates. FEBS J 272:1243-54.

1307 136. Yeats C, Finn RD, Bateman A. 2002. The PASTA domain: a beta-lactam-binding
1308 domain. Trends Biochem Sci 27:438.

1309 137. Osaki M, Arcondeguy T, Bastide A, Touriol C, Prats H, Trombe MC. 2009. The
1310 StkP/PhpP signaling couple in *Streptococcus pneumoniae*: cellular organization and
1311 physiological characterization. J Bacteriol 191:4943-50.

1312 138. Pallova P, Hercik K, Saskova L, Novakova L, Branny P. 2007. A eukaryotic-type
1313 serine/threonine protein kinase StkP of *Streptococcus pneumoniae* acts as a dimer in vivo.
1314 Biochem Biophys Res Commun 355:526-30.

1315 139. Sun X, Ge F, Xiao CL, Yin XF, Ge R, Zhang LH, He QY. 2010. Phosphoproteomic
1316 analysis reveals the multiple roles of phosphorylation in pathogenic bacterium *Streptococcus*
1317 *pneumoniae*. J Proteome Res 9:275-82.

- 1318 140. Novakova L, Bezouskova S, Pompach P, Spidlova P, Saskova L, Weiser J, Branny P.
1319 2010. Identification of multiple substrates of the StkP Ser/Thr protein kinase in *Streptococcus*
1320 *pneumoniae*. J Bacteriol 192:3629-38.
- 1321 141. Giefing C, Jelencsics KE, Gelbmann D, Senn BM, Nagy E. 2010. The pneumococcal
1322 eukaryotic-type serine/threonine protein kinase StkP co-localizes with the cell division apparatus
1323 and interacts with FtsZ *in vitro*. Microbiology 156:1697-707.
- 1324 142. Fleurie A, Cluzel C, Guiral S, Freton C, Galisson F, Zanella-Cleon I, Di Guilmi AM,
1325 Grangeasse C. 2012. Mutational dissection of the S/T-kinase StkP reveals crucial roles in cell
1326 division of *Streptococcus pneumoniae*. Mol Microbiol 83:746-58.
- 1327 143. Beilharz K, Novakova L, Fadda D, Branny P, Massidda O, Veening JW. 2012. Control of
1328 cell division in *Streptococcus pneumoniae* by the conserved Ser/Thr protein kinase StkP. Proc
1329 Natl Acad Sci U S A 109:E905-13.
- 1330 144. Falk SP, Weisblum B. 2013. Phosphorylation of the *Streptococcus pneumoniae* cell wall
1331 biosynthesis enzyme MurC by a eukaryotic-like Ser/Thr kinase. FEMS Microbiol Lett 340:19-
1332 23.
-  1333 145. Holeckova N, Doubravova L, Massidda O, Molle V, Buriankova K, Benada O,
1334 Kofronova O, Ulrych A, Branny P. 2014. LocZ is a new cell division protein involved in proper
1335 septum placement in *Streptococcus pneumoniae*. MBio 6:e01700-14.
-  1336 146. Saskova L, Novakova L, Basler M, Branny P. 2007. Eukaryotic-type serine/threonine
1337 protein kinase StkP is a global regulator of gene expression in *Streptococcus pneumoniae*. J
1338 Bacteriol 189:4168-79.
- 1339 147. Burnside K, Lembo A, Harrell MI, Gurney M, Xue L, BinhTran NT, Connelly JE, Jewell
1340 KA, Schmidt BZ, de los Reyes M, Tao WA, Doran KS, Rajagopal L. 2011. Serine/threonine

1341 phosphatase Stp1 mediates post-transcriptional regulation of hemolysin, autolysis, and virulence
1342 of group B Streptococcus. J Biol Chem 286:44197-210.

1343 ~~148.~~ Pompeo F, Foulquier E, Serrano B, Grangeasse C, Galinier A. 2015. Phosphorylation of
1344 the cell division protein GpsB regulates PrkC kinase activity through a negative feedback loop in
1345 *Bacillus subtilis*. Mol Microbiol 97:139-50.

1346 ~~149.~~ Straume D, Stamsas GA, Berg KH, Salehian Z, Havarstein LS. 2017. Identification of
1347 pneumococcal proteins that are functionally linked to penicillin-binding protein 2b (PBP2b). Mol
1348 Microbiol 103:99-116.


1349 ~~150.~~ Karimova G, Dautin N, Ladant D. 2005. Interaction network among *Escherichia coli*
1350 membrane proteins involved in cell division as revealed by bacterial two-hybrid analysis. J
1351 Bacteriol 187:2233-43.

1352 ~~151.~~ Massidda O, Anderluzzi D, Friedli L, Feger G. 1998. Unconventional organization of the
1353 division and cell wall gene cluster of *Streptococcus pneumoniae*. Microbiology 144 (~~Pt~~
1354 ~~11~~):3069-78.

1355 ~~152.~~ Claessen D, Emmins R, Hamoen LW, Daniel RA, Errington J, Edwards DH. 2008.
1356 Control of the cell elongation-division cycle by shuttling of PBP1 protein in *Bacillus subtilis*.
1357 Mol Microbiol 68:1029-46.

1358 ~~153.~~ Strahl H, Hamoen LW. 2012. Finding the corners in a cell. Curr Opin Microbiol 15:731-
1359 6.

1360 ~~154.~~ Rismondo J, Cleverley RM, Lane HV, Grosshennig S, Steglich A, Moller L, Mannala
1361 GK, Hain T, Lewis RJ, Halbedel S. 2016. Structure of the bacterial cell division determinant
1362 GpsB and its interaction with penicillin-binding proteins. Mol Microbiol 99:978-98.

- 1363 [155.](#) Cleverley RM, Rismondo J, Lockhart-Cairns MP, Van Bentum PT, Egan AJ, Vollmer W,
1364 Halbedel S, Baldock C, Breukink E, Lewis RJ. 2016. Subunit arrangement in GpsB, a regulator
1365 of cell wall biosynthesis. *Microb Drug Resist* 22:446-60.
- 1366 [156.](#) Wu LJ, Errington J. 2011. Nucleoid occlusion and bacterial cell division. *Nat Rev*
1367 *Microbiol* 10:8-12.
- 1368 [157.](#) Monahan LG, Liew AT, Bottomley AL, Harry EJ. 2014. Division site positioning in
1369 bacteria: one size does not fit all. *Front Microbiol* 5:19.
- 1370 [158.](#) Rowlett VW, Margolin W. 2015. The Min system and other nucleoid-independent
1371 regulators of Z ring positioning. *Front Microbiol* 6:478.
- 1372  ~~[159.](#) Fleurie A, Lesterlin C, Manuse S, Zhao C, Cluzel C, Lavergne JP, Franz-Wachtel M,
1373 Macek B, Combet C, Kuru E, VanNieuwenhze MS, Brun YV, Sherratt D, Grangeasse C. 2014b.
1374 MapZ marks the division sites and positions FtsZ rings in *Streptococcus pneumoniae*. *Nature*
1375 516:259-262.~~
- 1376 [160.](#) Manuse S, Jean NL, Guinot M, Lavergne JP, Laguri C, Bougault CM, VanNieuwenhze
1377 MS, Grangeasse C, Simorre JP. 2016a. Structure-function analysis of the extracellular domain of
1378 the pneumococcal cell division site positioning protein MapZ. *Nat Commun* 7:12071.
- 1379 [161.](#) van Raaphorst R, Kjos M, Veening JW. 2017. Chromosome segregation drives division
1380 site selection in *Streptococcus pneumoniae*. *Proc Natl Acad Sci U S A* 114:E5959-E5968.
- 1381 [162.](#) Manuse S, Fleurie A, Zucchini L, Lesterlin C, Grangeasse C. 2016b. Role of eukaryotic-
1382 like serine/threonine kinases in bacterial cell division and morphogenesis. *FEMS Microbiol Rev*
1383 40:41-56.

1384 **FIGURE LEGENDS**

1385

1386 **FIG. 1.** Diagrammatic sketch of the cell wall complex of pneumococci. Some of the MurNAc
1387 and GlcNAc residues in the glycan chains of peptidoglycan are modified by O-acetylation or N-
1388 deacetylation, respectively. Direct and indirect peptide cross-links are shown. Capsular
1389 polysaccharides have been assumed to be connected to MurNAc residues in peptidoglycan but
1390 recent work showed that they might be connected to GlcNAc residues. Surface proteins are
1391 covalently linked to peptides in peptidoglycan, choline-binding proteins attach non-covalently to
1392 phosphoryl choline residues in wall teichoic acid.

1393

1394 **FIG. 2.** Role of MurM and MurN in cell wall branching. The substrate of the MurM- and MurN-
1395 catalyzed branchin reaction is lipid II, which is composed of N-acetylated disaccharide units of
1396 glucosamine (hexagon with G) and muramic acid (hexagon with M) with the pentapeptide
1397 attached to the M residues. Lipid II is anchored on the plasma membrane through the carrier lipid
1398 bactoprenyl phosphate (the zig-zag line). Attachment of the completed precursor to the pre-
1399 existing cell wall occurs on the outer surface of the plasma membrane by the activity of
1400 glycosyltransferases and transpeptidases. Reproduced with permission from Ref (82).

1401

1402 **Figs 3A & B:** HPLC elution profiles of stem peptides of the peptidoglycan from the penicillin-
1403 susceptible strain R36A and several penicillin-resistant strains that carry different abnormal
1404 *murM* alleles. Structures of cell wall stem peptides identified in the pneumococcal peptidoglycan
1405 of penicillin-susceptible and –resistant strains of pneumococci. Reproduced with permission
1406 from Ref (42).

1407 **FIG. 4:** Structure of the pneumococcal lipoteichoic acid and wall teichoic acid. Both types of
1408 teichoic acid have identical chains (top part) which carry phosphoryl choline and D-alanine
1409 residues. In LTA the teichoic acid chains are β -glycosidically linked from AATGal to the lipid
1410 anchor (bottom left), in WTA the linkage occurs via an α -linkage from AATGal to MurNAc-
1411 phosphate in peptidoglycan. The figure was kindly provided by Nicolas Gisch (Research Centre
1412 Borstel, Germany).

1413

1414 **FIG. 5.** Cartoon of a cell wall growth and division complex at mid-cell showing elongation and
1415 cell division proteins, and the peptidoglycan hydrolases PcsB and LytB which cleave the septum
1416 for pole formation and cell separation.

1417

1418 **Table 1:** Cell wall peptide composition of several strains of *S. pneumoniae*. Reproduced with
1419 permission from Ref (78).

1420

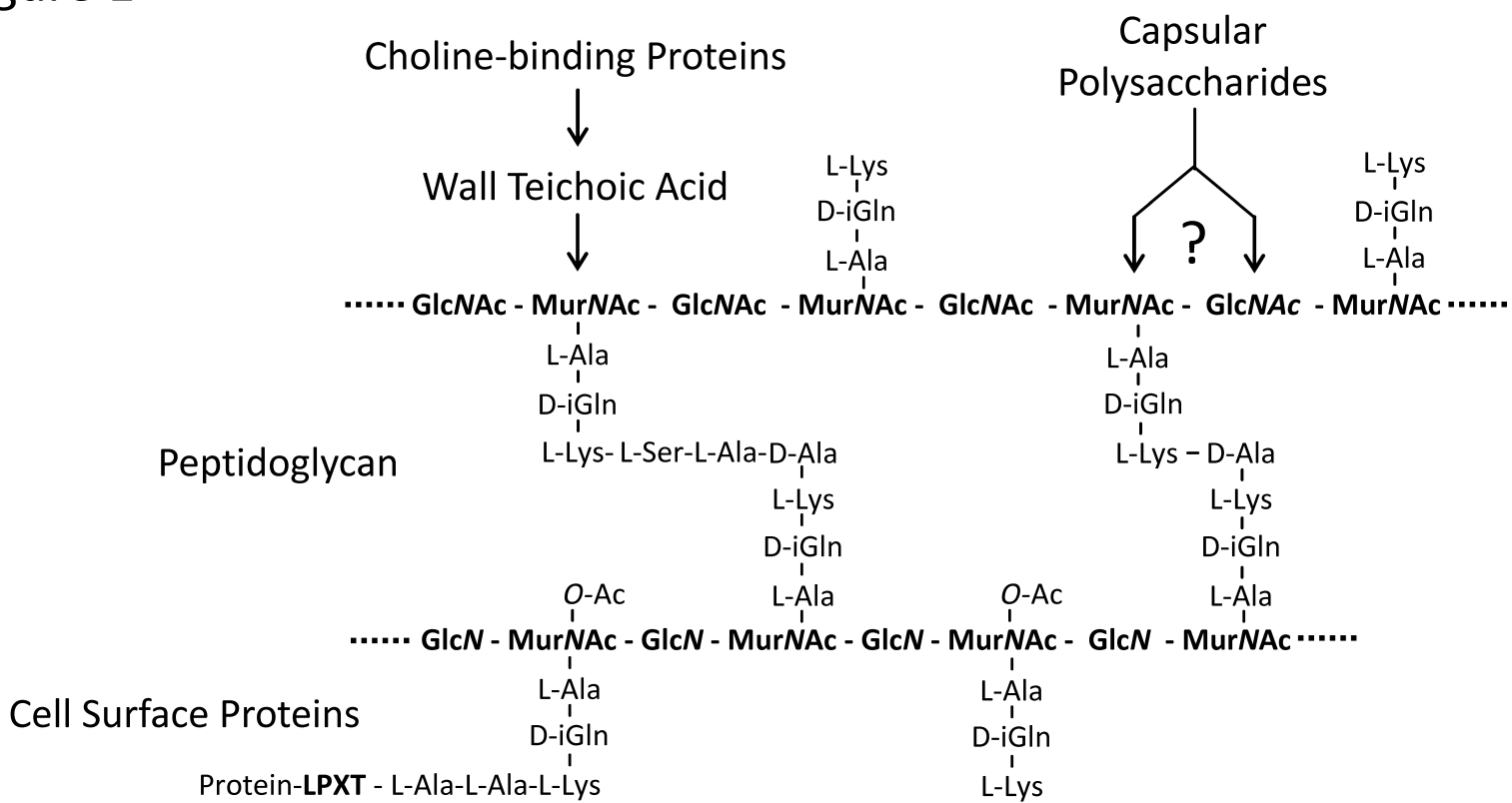
TABLE 1. Cell wall peptide composition of several strains of *S. pneumoniae*.

Peptide	% Peptide in				
	R36A (<i>murMA</i>)	Pen6 (<i>murMB2</i>)	Hun45 (<i>murMB1</i>)	DE1 (<i>murMB3</i>)	KY17 (<i>murMB5</i>)
1	13.3	2.6	4.5	10.8	3.4
2	3.4	0.7	0.5	1.4	0.6
3	2.8	14.3	7.2	1.0	28.5
I	1.8	14.4	24.1	23.4	11.2
II	3.4	2.7	5.1	3.1	0.8
4	21.0	3.2	4.4	6.0	7.2
III	1.3	3.5	6.7	6.9	2.1
5	12.7	2.2	0.9	0.5	2.9
6	7.1	2.5	2.8	9.3	1.9
7	7.4	11.1	1.4	0.4	19.7
IV	2.6	6.5	4.7	0.6	4.1
V	2.8	12.3	8.1	3.7	5.2
8	7.8	2.5	1.4	0.6	5.8
VI	6.6	10.1	19.1	27.5	2.0
9	6.0	11.6	9.0	4.9	4.5
Total	100	100	100	100	100
Monomers	26	38	48	47	47
Multimers	74	62	52	53	53
Linear	50	12	14	23	17
Branched	50	88	86	77	83
Branched/linear	1.0	7.4	6.4	3.3	4.9

1422

1423

Figure 1



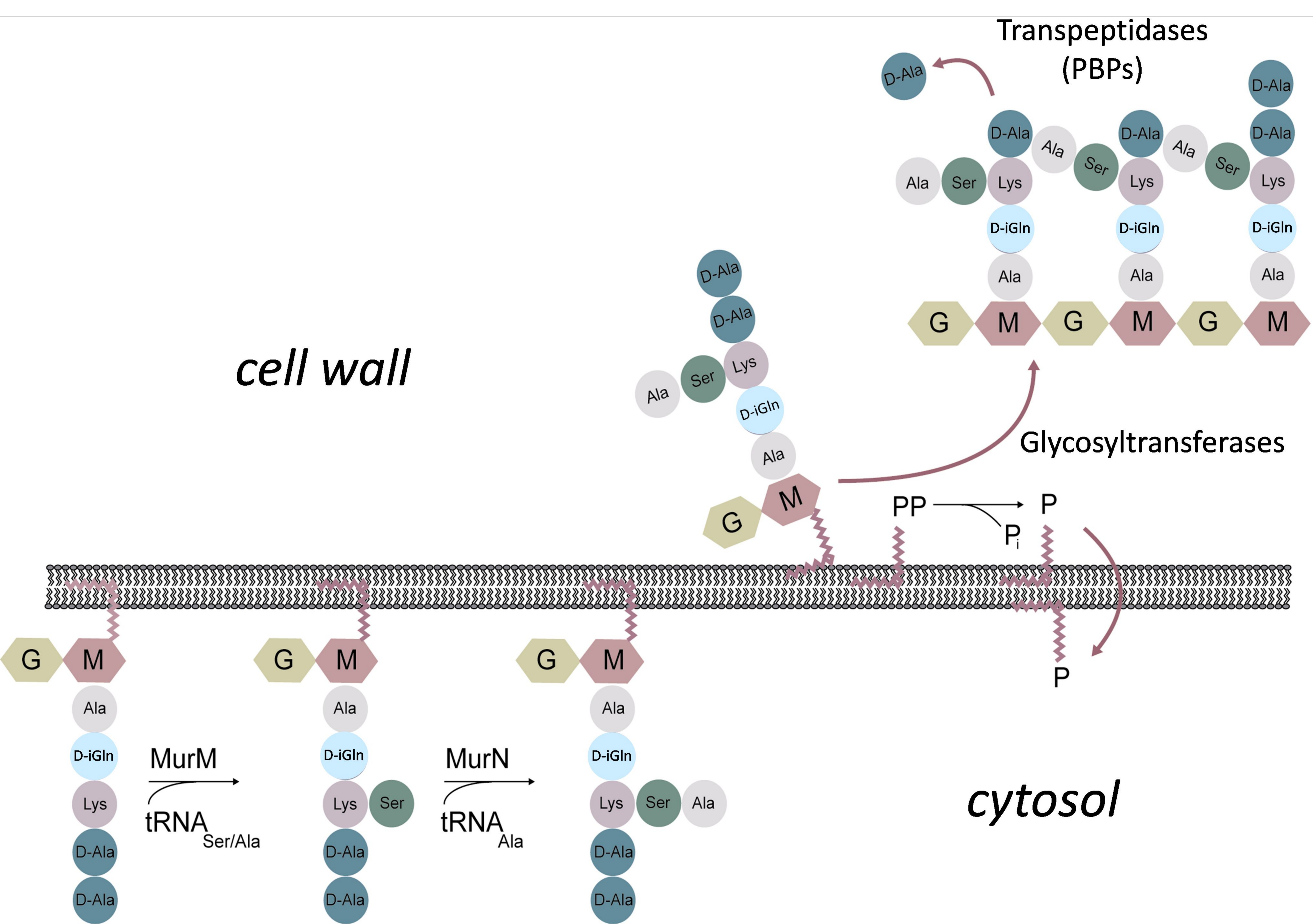
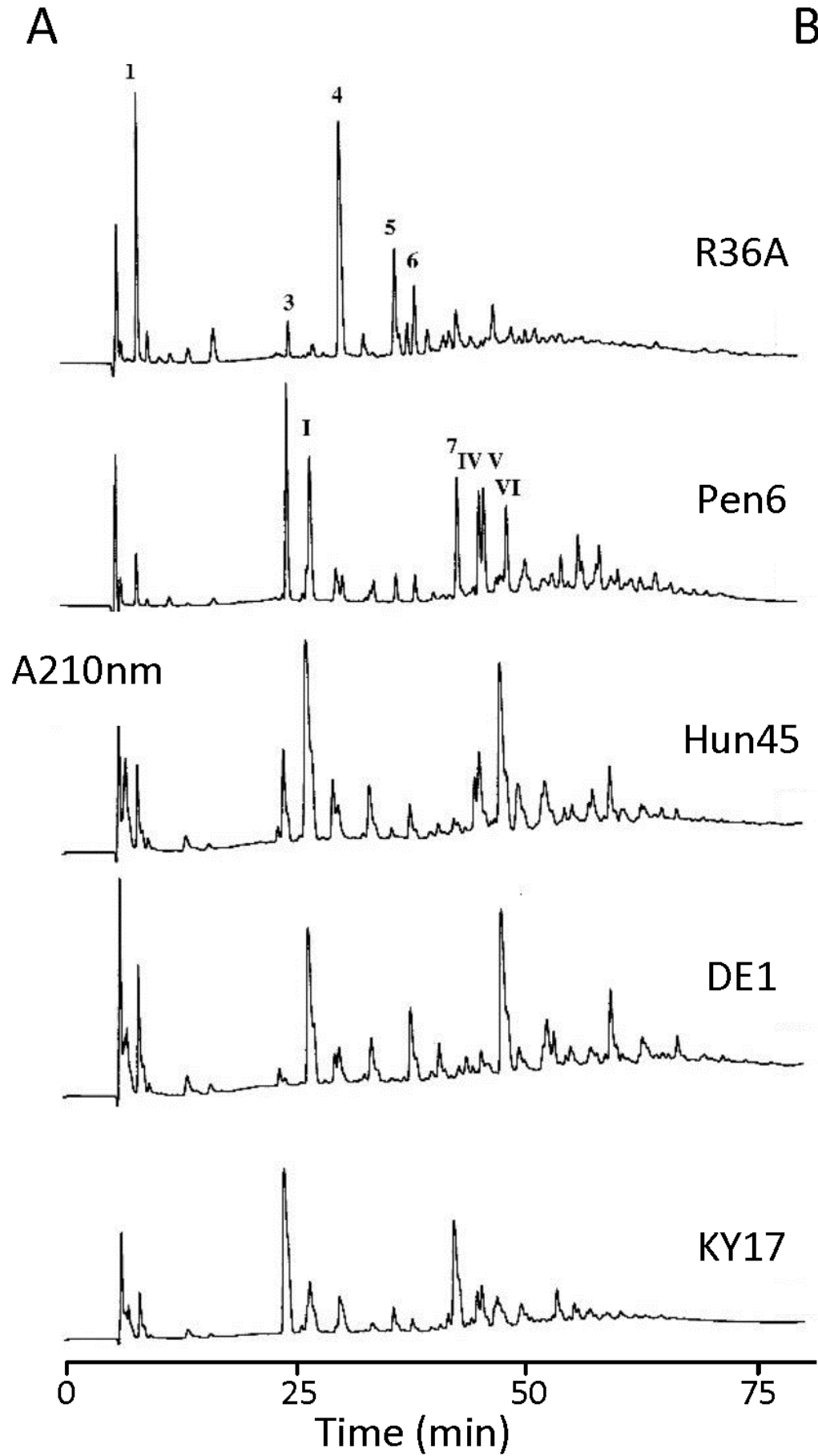


Figure 3



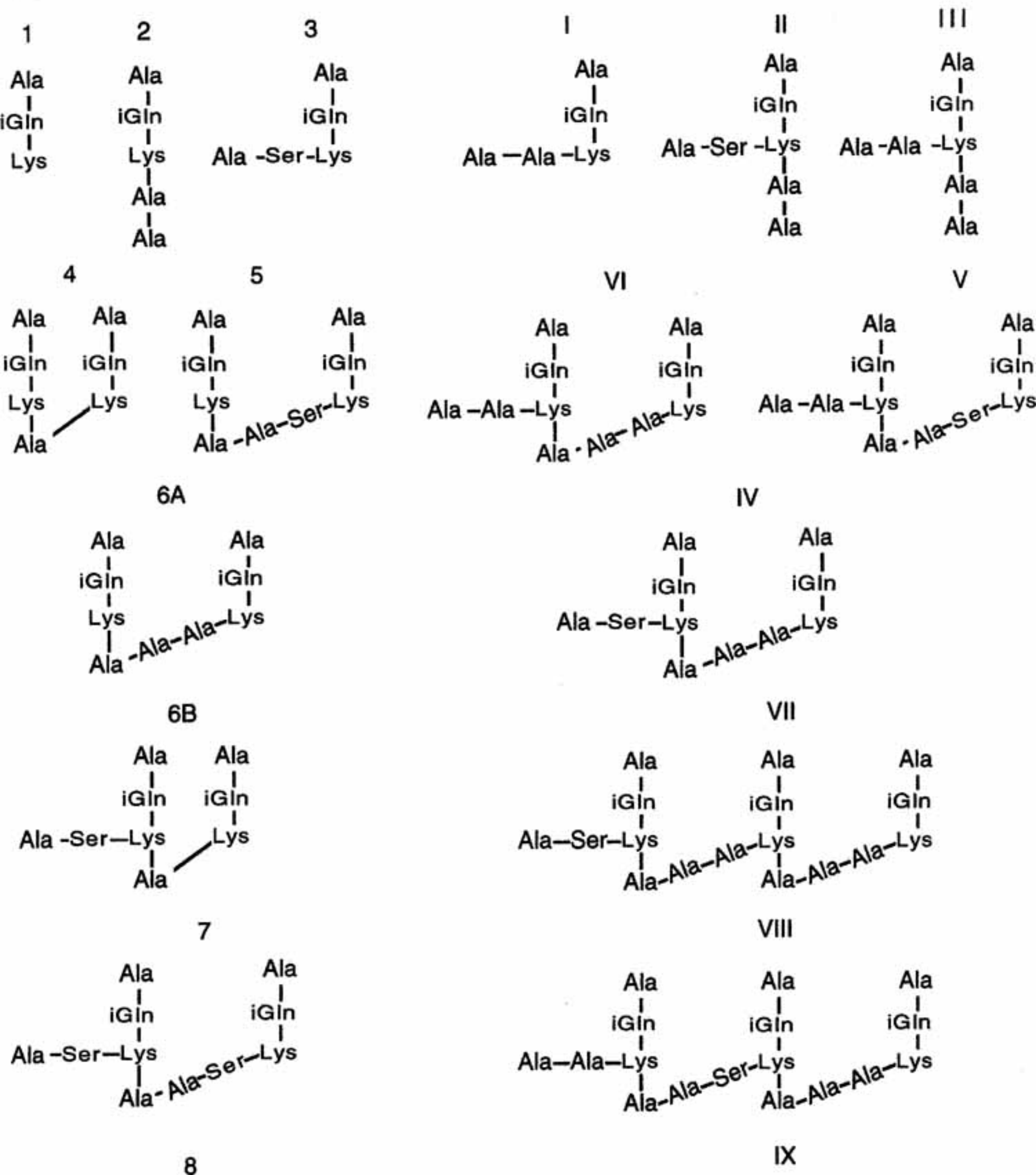
B

Figure 4

